

TabTreeFormer: Tabular Data Generation Using Hybrid Tree-Transformer

Jiayu Li^{1,2} Bingyin Zhao^{1,2} Zilong Zhao^{1,2} Kevin Yee² Uzair Javaid² Biplab Sikdar³

Abstract

Transformers have achieved remarkable success in tabular data generation. However, they lack domain-specific inductive biases which are critical to preserving the intrinsic characteristics of tabular data. Meanwhile, they suffer from poor scalability and efficiency due to quadratic computational complexity. In this paper, we propose TabTreeFormer, a hybrid transformer architecture that incorporates inductive biases of tree-based models (i.e., non-smoothness and non-rotational invariance) to process the potentially discrete and low-correlated patterns in tabular data, and hence enhances the fidelity and utility of synthetic data. In addition, we devise a novel tokenizer to capture the multimodal continuous distribution and further facilitate the learning of numerical value distribution. Moreover, our proposed tokenizer reduces the vocabulary size and sequence length based on the complexity of tabular data, shrinking the model size significantly without sacrificing the capability of the transformer model. We evaluate TabTreeFormer on 10 datasets against multiple generative models in various metrics; our experimental results show that TabTreeFormer achieves superior fidelity, utility, privacy, and efficiency. Our best model yields a 40% utility improvement with 1/16 of the baseline model size. Code is available at: <https://anonymous.4open.science/r/tabtreeformer-9585>.

1. Introduction

Tables are one of the most prevalent data modalities in real-world applications (e.g., healthcare (Dash et al., 2019), financial services (Assefa et al., 2021), etc.), yet are heavily under-exploited due to privacy concerns (EU, 2016). Fortunately, synthetic data offers an alternative to the utilization

¹Asian Institute of Digital Finance, National University of Singapore, Singapore, Singapore ²Betterdata AI, Singapore, Singapore ³Department of Electrical and Computer Engineering, National University of Singapore, Singapore, Singapore. Correspondence to: Jiayu Li <li.jiayu@nus.edu.sg>, Zilong Zhao <z.zhao@nus.edu.sg>.

Preliminary work. Do not distribute.

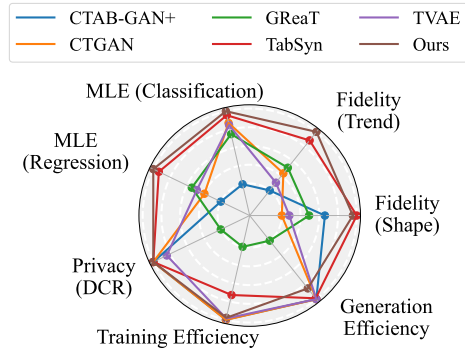


Figure 1. Performance comparison of TabTreeFormer (Ours) and other representative tabular generative models in terms of fidelity, utility (i.e., MLE), privacy, and efficiency. TabTreeFormer outperforms other models on almost all metrics.

of tabular data by modeling the characteristics of real data and reducing the risk of data breach (PDPC, 2024), thus drawing considerable attention in recent years.

State-of-the-art research shows that transformers such as autoregressive transformers (Borisov et al., 2023), masked transformers (Gulati & Roysdon, 2023), and diffusion models with transformers (Zhang et al., 2024) have achieved impressive fidelity, utility, and privacy in tabular data generation, allowing synthetic data to empower a variety of fields (Hernandez et al., 2022; Assefa et al., 2021). However, unlike the application of transformers in other research areas such as computer vision (Dosovitskiy et al., 2021) and natural language processing (Vaswani et al., 2017), existing transformer models for synthetic tabular data often overlook domain-specific priors (i.e., inductive biases). For example, CvT (Wu et al., 2021) introduces convolutional embedding and projection to transformers to boost vision performances, and Transformer-XL (Dai et al., 2019) introduces segment-level recurrence to transformers to capture longer-term dependencies in long text. While vision and language models have enjoyed the performance boost introduced by domain-specific priors, less exploration has been conducted to leverage them in tabular generative models. Moreover, transformers suffer from poor scalability due to quadratic computational complexity. This raises two interesting questions:

1. What inductive biases are beneficial to the fidelity and utility of synthetically generated tabular data?
2. How can one exploit unique characteristics of tabular

data to improve model scalability and efficiency?

To answer the questions, we propose TabTreeFormer, a generative hybrid transformer incorporating a tree-based model and a deliberately devised tokenizer to process and introduce tabular-specific inductive biases. We also leverage the limited per-dimension semantic meaning (i.e., each dimension corresponds to at most one feature) of typical tabular data to enable a significant reduction in model size by our tokenizer design.

Tree-based models excel at tabular classification and regression tasks (Shwartz-Ziv & Armon, 2022; Gorishniy et al., 2021), which is attributed to their inductive biases to capture tabular characteristics such as *non-smoothness* and potentially *low-correlation* (Grinsztajn et al., 2022). *Non-smoothness* is due to the existence of discrete features and non-smooth relations between discrete and/or continuous features. Tree-based models learn piece-wise constant functions rather than low-frequency functions (i.e., the functions neural networks tend to learn) (Rahaman et al., 2019), so that they are exceptionally good at capturing such non-smooth patterns. *textit{Low-correlated ifeatures}* include uninformative features that contribute trivially to downstream tasks such as classification and regression. Due to the non-rotationally invariant nature of tree-based models (Ng, 2004), trees are more robust against low-correlated features, while neural networks are biased towards stronger correlations. Inspired by the success of tree models on tabular tasks due to their inductive bias, we propose to employ such priors to facilitate the performance of tabular generative tasks.

However, tree models are not panaceas as they do not inherently capture *multimodal distribution* in continuous features (i.e., features with probability density functions possessing multiple modes/peaks), which is an essential challenge for tabular generative tasks. Inspired by the prior work (Xu et al., 2019) that tackles the challenge using multimodal decomposition, we propose dual-quantization tokenization for numeric values, a variant of multimodal decomposition catered for transformers where the first quantization is a K-Means (MacQueen, 1967) quantization that captures the multimodal distribution, and the second quantization is a quantile quantization for more precise representation of numerical values.

Moreover, we further optimize the tokenizer to significantly reduce vocabulary size and sequence length by considering the structured nature of tabular data and limited semantic meaning in each dimension (i.e., sole feature for each dimension). In addition, the limited complexity of training data in tables (compared to vision and language tasks) leads to room for reducing model complexity (e.g., hidden dimensions, number of heads, number of layers, etc.) and eventually slimming down the entire model size.

Our contributions are summarized as follows:

- To the best of our knowledge, we are the first work that introduces tabular-specific inductive biases to transformers to improve tabular generative models. We propose a novel hybrid transformer coupled with a tree-based model to bring in such inductive biases.
- We devise a dual-quantization tokenizer that models the multimodal distribution of continuous values. This practice facilitates learning of numerical distribution and further improves the quality of synthetic data.
- Employing the characteristics of tabular data, our tokenizer design also leads to a much smaller vocabulary size and sequence length, achieving a phenomenal model size reduction and efficiency enhancement.
- We evaluate TabTreeFormer across 10 datasets against 8 representative tabular generative models and show that TabTreeFormer outperforms other models in fidelity, utility, privacy, and efficiency, as shown in Fig. 1. Notably, with just 1/16 of the baseline model size, our best model achieves a 40% utility improvement over the best-performing baseline model.

2. Related Works

2.1. Tabular Data Generation

Early works on tabular data generation predominantly utilized MLPs and CNNs as backbone architectures and GAN and VAE as generation methods (Park et al., 2018; Xu et al., 2019; Zhao et al., 2021; 2024). Recent works evolved to use transformers with auto-regression, masked modeling, and diffusion as generative paradigms (Borisov et al., 2023; Zhang et al., 2024; Gulati & Roysdon, 2023). For example, TabMT (Gulati & Roysdon, 2023) employs a masked transformer with ordered embedding and achieves outstanding utility in downstream tasks with improved scalability, and TabSyn (Zhang et al., 2024) encodes tabular data into a latent space and generates tabular data using diffusion model, demonstrating impressive fidelity and utility. Despite their enhanced performance, these works overlook the essential inductive biases to capture non-smoothness and low-correlated features that are crucial to preserving the intrinsic characteristics of tabular data.

Xu et al. (2019) finds that multimodal distribution in continuous features is a critical aspect for tabular generative models' inductive bias to capture. CTGAN (Xu et al., 2019) uses variational Gaussian mixture model (Bishop, 2006) to decompose multimodal values while TabDiff (Shi et al., 2024) introduces a multimodal stochastic sampler. In this work, we devise a tokenizer that models the multimodal distribution and introduces the prior into the auto-regressive transformer.

2.2. Tree-based Models for Tabular Data

Tree-based gradient boosting algorithms are the dominant approach for tabular tasks, notable examples are XGBoost (Chen & Guestrin, 2016), LightGBM (Ke et al., 2017), and CatBoost (Prokhorenkova et al., 2018). These tree-based models are ensembles of small and intuitive decision trees that naturally understand feature relations and interactions, thus achieving high predictive performance, efficiency, and scalability. Although recent research has shown promise of transformers in tabular data-related tasks (Huang et al., 2020; Arik & Pfister, 2021; Hollmann et al., 2023), their suboptimal performance caused by the absence of tabular-specific inductive biases makes them still less favorable to tree-based models in many scenarios (Shwartz-Ziv & Armon, 2022; Gorishniy et al., 2021). Meanwhile, tree-based generative models (Watson et al., 2023; McCarter, 2024), while being efficient, still fall short of synthetic data quality compared to deep neural networks like transformers. In this work, we take advantage of both models and employ tree-based models to introduce tabular-specific inductive bias and facilitate the learning of the transformer model.

2.3. Tokenizers for Tabular Data

Transformers are not originally designed for tabular data, entailing a need for a tokenizer to translate tabular data to transformer-friendly input tokens or embeddings. Arik & Pfister (2021); Zhang et al. (2024) translate tabular data into a continuous space by completely reformulating the tokenization and embedding layers. Borisov et al. (2023); Solatorio & Dupriez (2023); Gulati & Roysdon (2023) translate tabular data to a sequence of tokens (i.e., discrete space) by a tabular-specific tokenization method, and retain the embedding layer with moderate modifications, which is akin to natural language and more suitable for transformers. In this paper, we opt for the second choice to optimize the tokenizer for tabular data.

3. TabTreeFormer

Recall that our goal is to improve the performance and efficiency of the generative model by introducing domain-specific inductive biases and shrinking the model size. Formally, let \mathbf{X} be the tabular training dataset for a generative model with n rows, m_d discrete and m_c continuous features, we aim to generate synthetic tabular data \mathbf{X}' similar to \mathbf{X} . To achieve this, we propose TabTreeFormer that consists of three building blocks: a tree-based model, a tokenizer, and a transformer model, as shown in Fig. 2. The tree-based model captures some tabular-specific inductive biases, and the tokenizer is used to grasp the multimodal distribution while reducing vocabulary size and sequence length simultaneously. The transformer model learns the priors extracted from the tree-based model and tokenizer to produce high-

Algorithm 1 Training of TabTreeFormer

```

1: Input: Tabular dataset  $\mathbf{X}$  ( $n$  rows,  $m_d$  discrete features,  $m_c$  continuous features),  $s$  total training steps
2: Output: Fitted tree-based model  $\mathcal{T}$  and the leaf index matrix  $\mathbf{J}$ , data tokenizer  $\mathcal{D}$ , and transformer  $\mathcal{G}$ 
3:  $\mathcal{T} \leftarrow \text{TUNEHYPERPARAMANDFITTREEBASEDMODEL}(\mathbf{X})$ 
   ▶ Let  $T = \mathcal{T}.\text{N\_TREES}$ ,  $n_l = \mathcal{T}.\text{MAX\_N\_LEAVES}$ 
4:  $\mathbf{J} \leftarrow \mathcal{T}.\text{GETLEAFINDEX}(\mathbf{X})$ 
   ▶ Obtain leaf index matrix  $\mathbf{J} \in \mathbb{N}^{n \times T}$ 
5:  $\mathcal{D} \leftarrow \text{FITENCODER}(\mathbf{X})$ 
   ▶  $n_c = \mathcal{D}.\text{MAX\_N\_CAT}$ ,  $n_b = \mathcal{D}.\text{MAX\_N\_BIN}$ ,  $n_q = \mathcal{D}.\text{MAX\_N\_QUANT}$ 
6:  $\tilde{\mathbf{X}} \leftarrow \mathcal{D}.\text{ENCODE}(\mathbf{X})$ 
   ▶ Get cat/bin/quant IDs  $\tilde{\mathbf{X}} \in \mathbb{N}^{n \times (m_d + 2m_c)}$ 
7:  $\mathbf{Z} \leftarrow \text{TOTOKENIDS}([\mathbf{J}; \tilde{\mathbf{X}}])$ 
   ▶ Convert these IDs to token IDs, add BOS, EOS
8:  $\mathcal{G} \leftarrow \text{INITIALIZELM}(n_{\text{pos}} = 2 + T + m_d + 2m_c, n_{\text{vocab}} = 3 + n_l + n_c + n_b + n_q)$ 
9: for  $i = 1, \dots, s$  do
10:    $\mathbf{B} \leftarrow \text{SAMPLEBATCH}(\mathbf{Z})$ 
11:    $\tilde{\mathbf{B}} \leftarrow \text{MASK}(\mathbf{B})$ 
12:    $\mathcal{G} \leftarrow \text{UPDATEGRADIENT}(\text{input} = \tilde{\mathbf{B}}, \text{target} = \mathbf{B})$ 
13: end for

```

Algorithm 2 Tabular data generation using TabTreeFormer

```

1: Input: Leaf index matrix  $\mathbf{J}$ , data tokenizer  $\mathcal{D}$ , transformer-based language model  $\mathcal{G}$ , and number of rows generate  $n'$ 
2: Output: Synthetic tabular dataset  $\mathbf{X}'$ 
3:  $\mathbf{J}' \leftarrow \text{SAMPLE}(\mathbf{J}, n')$ 
4:  $\mathbf{Z}' \leftarrow \text{MASK}(\text{TOTOKENIDS}(\mathbf{J}'))$ 
5:  $\tilde{\mathbf{X}}' \leftarrow \mathcal{G}.\text{GENERATE}(\text{partial\_input} = \mathbf{Z}')$ 
6:  $\mathbf{X}' \leftarrow \mathcal{D}.\text{DECODE}(\tilde{\mathbf{X}}')$ 

```

quality synthetic data. Concrete accounts of training and generation algorithms are described in Algorithm 1 and 2.

3.1. Tree-based Models

To introduce tabular-specific inductive biases, we incorporate tree-based models into the transformer (“Tree-based Model” in Fig. 2). This is achieved by augmenting each token sequence representing one table row with additional information derived from the leaf indices of a tree-based model fitted on the prediction task defined on the dataset or a random feature if such a task is unavailable. Formally, let the fitted tree-based model be \mathcal{T} with T trees. Let $l_i \in \mathbb{N}$ be the number of leaves in i -th tree, where $i \in \{1, 2, \dots, T\}$. In tree \mathcal{T} , there is a *leaf index matrix* $\mathbf{J} = [j_{ik}] \in \mathbb{N}^{n \times T}$ of \mathbf{X} where $j_{ik} \in \{1, 2, \dots, l_k\}$ represents the leaf index of i -th row \mathbf{X}_i in the k -th tree. Leaf indices provide flattened positional information of each row in a tree, and hence inherently introduce the non-smooth and non-rotationally invariant inductive biases of trees to capture the *non-smoothness* and *potentially low-correlations* of tabular data. With leaf indices prepended to actual data values, although the subsequent model is still a neural network, tabular-specific inductive biases from tree-based models are inherited by the entire generative model through the construction of the intermediate input token sequence (i.e., indicated by the red

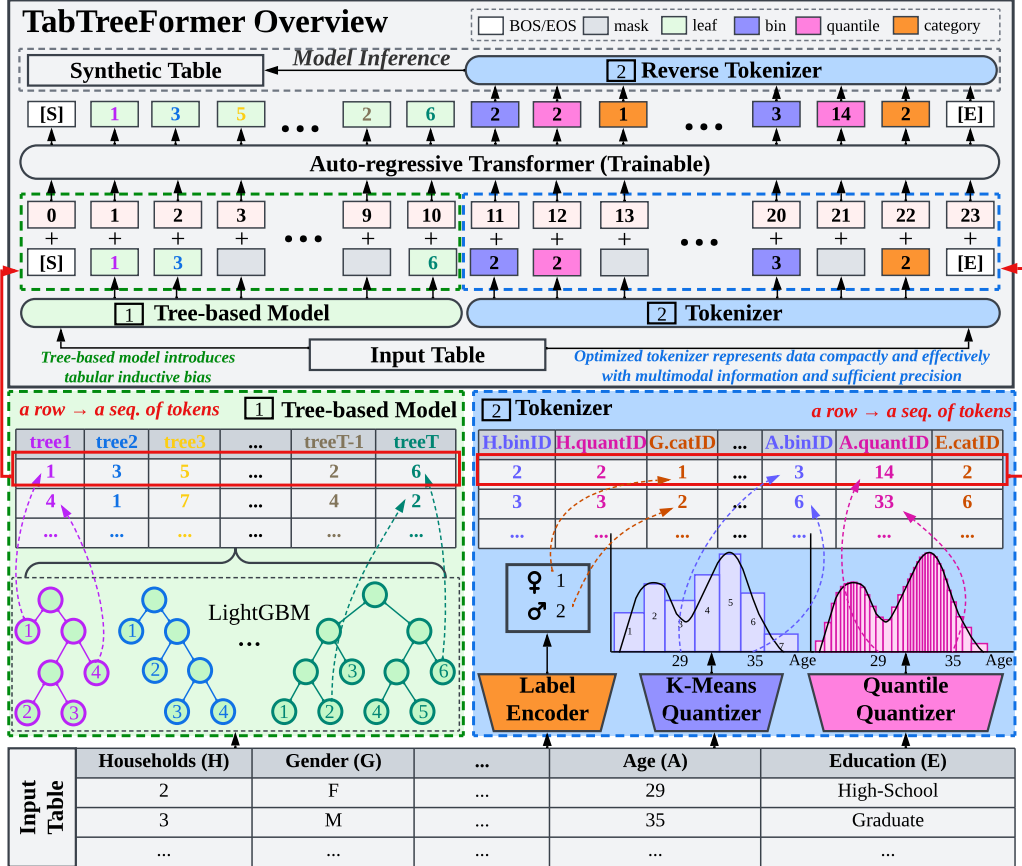


Figure 2. Overview of TabTreeFormer (data flow from bottom to top). TabTreeFormer consists of 3 components: i) a **tree-based model** that introduces tabular-specific inductive biases; ii) a **tokenizer** that efficiently and compactly represents data while capturing multimodal distributions; iii) a **transformer model** that learns the priors extracted from the tree and tokenizer to generate high-quality synthetic data.

arrows in Fig. 2), thereby improving the quality of the synthetic data. Leaf indices are also served as prompts during inference, allowing indirect yet informative hints to generate more realistic data.

3.2. Tokenizer

To model the multimodal distribution of continuous values and reduce the vocabulary size along with the tokenized input sequence length to eventually reduce the model size, we devise a tailored data tokenizer for tabular data (“Tokenizer” in Fig. 2). For each continuous feature, we quantize the values so that it is of a more natural data format for transformers to learn. However, unlike TabMT (Gulati & Roysdon, 2023) that uses a single quantizer, we use a dual-quantizer (i.e., double quantizers) to capture multimodal continuous distribution and describe the precise values respectively. Transformers do not expect near-Gaussian-distributed input tokens, so we capture the multimodal distribution simply by a K-Means quantizer (MacQueen, 1967) with a small number of clusters (e.g., $K = 10$). Following that, the original value is then quantized into a large number of quantiles (e.g., $Q = 1000$), based on which original values are recovered, and thus the values are highly precise.

Employing the dual-quantization tokenization scheme, each numeric value is encoded into two discrete values: a bin ID in the K-Means quantizer and a quantile ID in the quantile quantizer, allowing two tokens to represent a numeric value with valuable and sufficient information. Categorical features are simply tokenized by label encoding, requiring 1 token. Formally, a reversible data tokenizer \mathcal{D} can be fitted on \mathbf{X} . Let $c_i \in \mathbb{N}$, $b_i \in \{0, 1, \dots, K\}$, $q_i \in \{0, 1, \dots, Q\}$ denote the number of categories, K-Means bins, and quantiles per column respectively, where $c_i = 0$ in continuous features and $b_i = q_i = 0$ in categorical features. Then, the domain for a categorical value is $\{1, 2, \dots, c_i\} \subseteq \mathbb{N}^+$, and the domain for a continuous value is $\{1, 2, \dots, b_i\} \times \{1, 2, \dots, q_i\} \subseteq (\mathbb{N}^+)^2$.

3.3. Auto-regressive Transformer

TabTreeFormer is simply trained as an auto-regressive transformer. The input token sequence is constructed by concatenating the outcome from the tree model and tokenizer. It requires 5 types of tokens and a vocabulary size of $V = n_l + n_c + n_b + n_q + 3$. The number of tokens in a sequence corresponding to one row is $L = 2 + T + m_d + 2m_c$, including BOS and EOS tokens. Both the vocabulary size

Table 1. Illustration of tokens in TabTreeFormer. “Size” indicates the number of tokens belonging to this type. Recall Figure 2 for the colors and usage of them. “N” in “Format” column can be any index in the range. For example, leaf 3 ($3 < n_l$) is thus represented as [leaf3], corresponding to the light green tokens in Figure 2 with value 3.

Type (Alias)	Size	Format	Source	Description
Leaf	$n_l = \max_{i \in \{1, 2, \dots, T\}} l_i$	[leafN]	Tree-based model \mathcal{T}	Leaf index in a tree
Categorical (cat)	$n_c = \max_{i \in \{1, 2, \dots, n\}} c_i$	[catN]	Data tokenizer \mathcal{D} (categorical columns)	Category ID
Cluster (bin)	$n_b = \max_{i \in \{1, 2, \dots, n\}} b_i$	[binN]	Data tokenizer \mathcal{D} (numeric columns)	Bin ID in K-Means quantizer
Quantile (quant)	$n_q = \max_{i \in \{1, 2, \dots, n\}} q_i$	[quantN]	Data tokenizer \mathcal{D} (numeric columns)	Quantile ID in quantile quantizer
Special	3	[BOS] [EOS] [mask]	Classical special tokens for LMs	BOS, EOS, and mask tokens

and sequence length are much smaller than the need for natural language models. A shared set of leaf tokens across all trees and similarly shared sets of category, bin, and quantile tokens across all features are used. Distinctions between different trees and features are effectively encoded through positional information, leveraging the positional embeddings inherent in most transformers.

A key observation on the construction of token sequence is that the valid range of tokens at each position is fixed for a given table. Consequently, tokens can be sampled exclusively from this precomputed set of valid options during generation. This ensures that every generated token sequence corresponds to a valid row, eliminating the need for rejecting invalid sequences (Borisov et al., 2023; Solatorio & Dupriez, 2023; Zhao et al., 2023), thus significantly accelerating the sampling process.

Additionally, transformers are prone to memorization, particularly when trained on tabular data, where datasets are much smaller compared to typical natural language corpora (Borisov et al., 2023). To avoid memorization, we heavily mask the input and maintain the target output unmasked. The rest of the training and generation settings are similar to the training and generation of classical causal language models, except for a modified loss function to account for the ordinal relations between quantile tokens, with details introduced in Section 3.4.

3.4. Loss Function

We use cross-entropy loss (CEL) as the optimization objective of the transformer. However, the quantized quantile tokens retain an inherent ordinal property, where closer IDs correspond to closer values. This relationship is not captured by standard CEL, which treats all classes as equally distinct. To address this, we replace the vanilla CEL with a specialized ordinal CEL for quantile tokens.

Formally, let the predicted logits for a token be $\mathbf{z} \in \mathbb{R}^V$, the probability after softmax be $\mathbf{p} \in [0, 1]^V$ ($\|\mathbf{p}\|_1 = 1$), and let $t \in \{1, \dots, V\}$ be the target label. Recall the classical definition of CEL as given in Equation 1.

$$\mathcal{L}_{ce}(\mathbf{z}, t) = -\log \frac{e^{z_t}}{\sum_{i=1}^V e^{z_i}} = -\log p_t \quad (1)$$

We define *ordinal cross-entropy loss* (OCEL) as a variant of CEL where each term is weighted. These weights are applied to unnormalized probabilities in both the numerator and denominator, depending on the current- and target-class pairs. It contrasts with the classical weighted CEL, which weights the loss per class based solely on the target class and applies to the numerator only. Formally, we write it as Equation 2, where w_{ti} denotes the weight for z_i , where t is the target class.

$$\mathcal{L}_{oce}(\mathbf{z}, t) = -\log \frac{w_{tt} e^{z_t}}{\sum_{i=1}^V w_{ti} e^{z_i}} \quad (2)$$

Lemma 1. *Given $\mathbf{w} > \mathbf{0}$ not dependent on \mathbf{z} , OCEL is optimized when $z_t \rightarrow \infty$ and $z_i \rightarrow -\infty, \forall i \neq t$.*

Theorem 1. *Let $f(|t - i|)$ be a variant of the distance between current class i and target class t when f is non-negative and monotonically increasing. Let the weighted sum of this variant of distances to target incurred by some logit \mathbf{z} be $D(\mathbf{z}) = \sum_{i=1}^V p_i w_i$. If $w_{ti} = f(|t - i|)$ for some f , then for \mathbf{z}, \mathbf{z}^* with $\mathcal{L}_{ce}(\mathbf{z}, t) = \mathcal{L}_{ce}(\mathbf{z}^*, t)$ and $D(\mathbf{z}) < D(\mathbf{z}^*)$, we must have $\mathcal{L}_{oce}(\mathbf{z}, t) < \mathcal{L}_{oce}(\mathbf{z}^*, t)$.*

Both Lemma 1 and Theorem 1 are intuitive, and we provide rigorous proofs in Appendix A.1-A.2. Theorem 1 implies that the OCEL penalizes (value being smaller) classes closer to the target class less than farther ones. Any definition of $w_{ti} = f(|t - i|)$ satisfying the monotonicity constraint works for OCEL technically. In this paper, we define the weight w_{ti} for z_i to be obtained by Equation 3.

$$w_{ti} = 1 + m - e^{-\frac{(t-i)^2}{(V\sigma)^2}} \quad (3)$$

where $\sigma = 0.005$ is a scaling factor of the distance, and $m = 0.5$ is the minimum weight (used on $i = t$). Detailed explanation and analysis of it can be found in Appendix A.3.

Note that not all tokens are part of the ordinal relation, so the OCEL is applied only to valid quantile tokens at the corresponding positions. To enable the model to learn to generate valid quantile tokens, we introduce an additional modified CEL to distinguish valid tokens from invalid ones, which complements OCEL. Formally, let valid quantile tokens have IDs in the range $[Q_s, Q_e]$. The valid token group loss (for quantile tokens at this position) is defined by Equation 4 when $t \in [Q_s, Q_e]$.

$$\mathcal{L}_{vg}(\mathbf{z}, t) = -\log \frac{\sum_{i \in [Q_s, Q_e]} e^{z_i}}{\sum_{i=1}^V e^{z_i}} \quad (4)$$

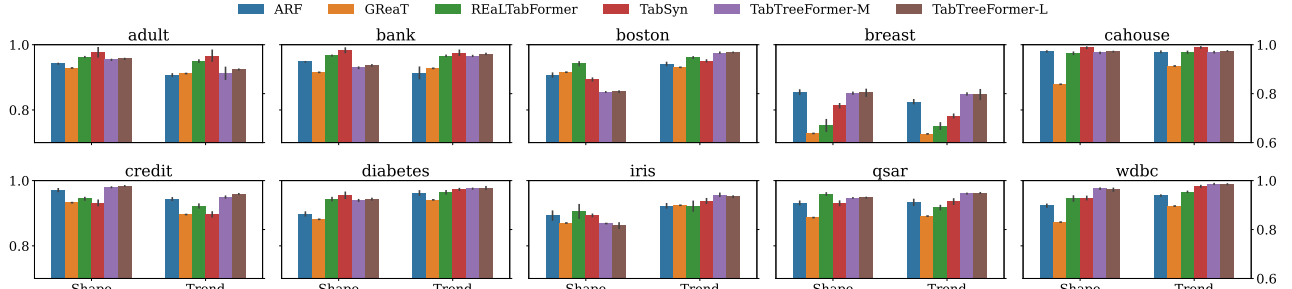


Figure 3. Performance comparison between different models in terms of fidelity. The higher the values are, the better the fidelity is. Top-4 performing baselines by fidelity mean scores are visualized.

In sum, Equation 5 expresses the loss function on one token.

$$\begin{aligned} & \mathcal{L}(\mathbf{z}, t) \\ &= \begin{cases} \mathcal{L}_{ce}(\mathbf{z}, t) & \text{if } t \notin [Q_s, Q_e] \\ \mathcal{L}_{oce}(\mathbf{z}_{Q_s:Q_e}, t - Q_s) + \mathcal{L}_{vg}(\mathbf{z}, t) & \text{if } t \in [Q_s, Q_e] \end{cases} \end{aligned} \quad (5)$$

Although the ordinal property also holds for K-Means bin IDs, we do not calculate the loss on them this way because the number of different bins is small, and we expect the model to predict the bins accurately.

4. Experiments

4.1. Experimental Setup

We conduct all experiments on NVIDIA RTX 4090. We use LightGBM (Ke et al., 2017) whose hyperparameters are tuned by Optuna (Akiba et al., 2019) as the tree-based model. We exploit Distill-GPT2 (Sanh et al., 2019) as the transformer backbone, following the practice in prior works (Borisov et al., 2023; Solatorio & Dupriez, 2023). TabTreeFormer (TTF) has three configurations: S (small), M (medium), and L (large), with the number of trainable parameters of approximately 1M, 5M, and 40M, respectively. Implementation and setting details can be found in Appendix B and Appendix C.1.

Datasets. Experiments are conducted on 10 datasets with diverse sizes and characteristics from OpenML (Vanschoren et al., 2013): adult, bank, boston, breast, cahouse, credit, diabetes, iris, qsar, and wdbc. Details of these datasets are summarized in Appendix C.2.

Baseline models. We compare the performance of TabTreeFormer against several influential and high-performing methods in tabular data generation including non-neural networks, GANs, VAEs, diffusion models, and auto-regressive transformers: ARF (Watson et al., 2023), CTAB-GAN+ (CTAB+) (Zhao et al., 2024), CTGAN (Xu et al., 2019), TVAE (Xu et al., 2019), TabDDPM (Kotelnikov et al., 2023), TabSyn (Zhang et al., 2024), GReAT (Borisov et al., 2023) and REaLTabFormer (RTF) (Solatorio & Dupriez, 2023). Implementation of baselines is described in Appendix C.3.

Metrics. We comprehensively evaluate TabTreeFormer us-

ing fidelity, utility, privacy, and efficiency, which are standard metrics in tabular data generation (Xu et al., 2019; Zhao et al., 2024; Borisov et al., 2023; Zhang et al., 2024; Shi et al., 2024). Detailed implementation of the metrics can be found in Appendix C.4-C.7.

- **Fidelity** shows the cosmetic discrepancy between the real and synthetic data. It is evaluated via “Shape” and “Trend” metrics (Dat, 2023; Shi et al., 2024). “Shape” measures the similarity of marginal distribution density for each column, and “Trend” measures the fidelity in correlation between column pairs. Higher “Shape” and “Trend” values indicate better data fidelity.
- **Utility** exhibits the quality of synthetic data by testing its performance on downstream tasks. We evaluate based on the established Train-on-Synthetic, Test-on-Real (TSTR) machine learning efficacy (MLE) evaluation framework (Xu et al., 2019), namely, synthetic data generated based on real training data is tested on a hold-out real test set. Three models are used: linear (i.e., linear and logistic regression; LN), random forest (RF) (Breiman, 2001), and XGBoost (XGB) (Chen & Guestrin, 2016). Classification performance is evaluated by weighted AUC ROC and regression is evaluated by R^2 . For both metrics, better generative models tend to yield higher scores on downstream tasks.
- **Privacy** is a crucial criterion when the synthetic data serves the use case of privacy-preserving data sharing. We use the distance to the closest record (DCR) (Zhao et al., 2021) to evaluate the privacy of synthetic data. We compare the DCR from synthetically generated data and from hold-out real (test) data to the real training data and privacy preservation is demonstrated by DCRs calculated on the latter being no smaller than the former, tested by Mann-Whitney U Test (Mann & Whitney, 1947). Privacy is at risk when p -values are smaller than 0.05.
- **Efficiency** showcases the model sizes and computation time for training and generation of different models. Under comparable performance, smaller models and faster computation are favored.

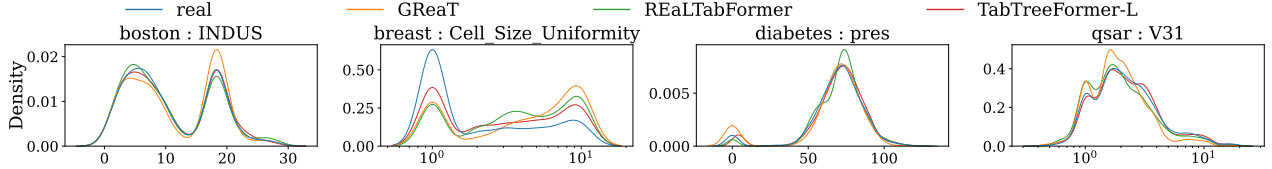


Figure 4. Comparison of marginal densities for generated data from baseline tabular auto-regressive transformers and TabTreeFormer against real data on representative multimodal continuous columns. All models use Distill-GPT2 as the backbone.

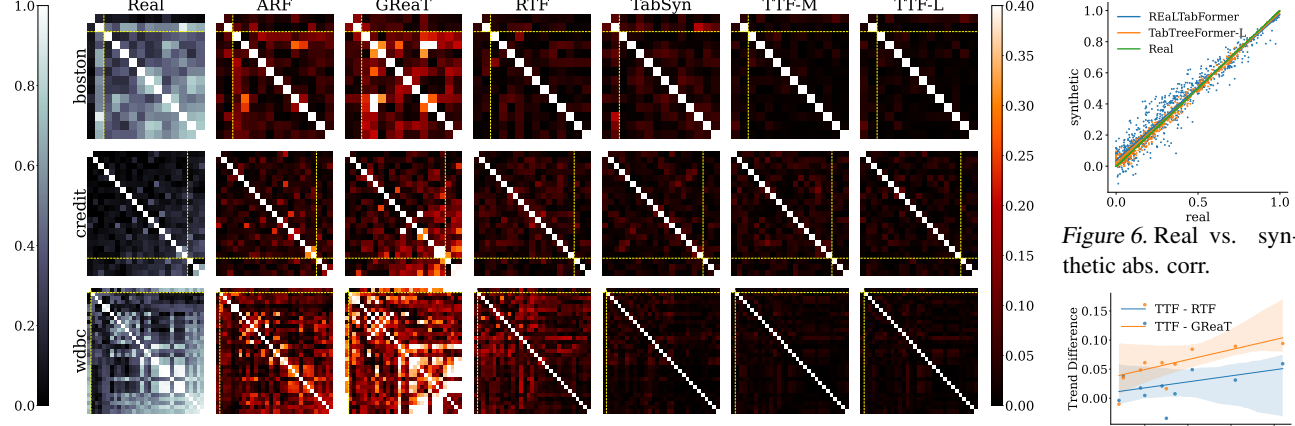


Figure 5. Performance comparison of TabTreeFormer versus top-4 performing baselines in fidelity on pair-wise correlation in 3 experimented datasets. Real (absolute) correlation values are presented on the left, and the absolute error in correlation values in synthetic data from different models, capped at 0.4 for better visibility, are shown at the right (the darker, the better). The left-top features are categorical features, and the right-bottom features are numeric features.

Table 2. MLE performance between different models. The top two rows calculate the global average scores and relative error (w.r.t real data). The middle three rows show the average performance in each ML model, and the bottom two rows show the average performances in classification (clf.) and regression (reg.). Classification tasks are evaluated by weighted AUC ROC scores, and regression tasks are evaluated by R^2 scores. The best scores and the second best scores are highlighted in bold with and without underscore, respectively.

	ARF	CTAB+	CTGAN	TabDDPM	GReaT	RTF	TabSyn	TVAE	TTF-S	TTF-M	TTF-L
Avg. (\uparrow)	0.843 ± 0.155	0.680 ± 0.271	0.810 ± 0.189	0.552 ± 0.865	0.800 ± 0.206	0.866 ± 0.130	0.865 ± 0.123	0.813 ± 0.189	0.863 ± 0.127	0.878 ± 0.113	0.880 ± 0.111
RE (\downarrow)	0.057 ± 0.077	0.244 ± 0.274	0.099 ± 0.137	0.483 ± 1.214	0.110 ± 0.170	0.027 ± 0.040	0.027 ± 0.029	0.095 ± 0.142	0.029 ± 0.040	0.017 ± 0.023	0.016 ± 0.023
LN (\uparrow)	0.835 ± 0.176	0.686 ± 0.258	0.810 ± 0.193	0.570 ± 0.882	0.800 ± 0.197	0.851 ± 0.153	0.849 ± 0.156	0.814 ± 0.163	0.853 ± 0.154	0.861 ± 0.145	0.862 ± 0.143
RF (\uparrow)	0.842 ± 0.156	0.681 ± 0.273	0.806 ± 0.200	0.566 ± 0.910	0.798 ± 0.220	0.873 ± 0.122	0.872 ± 0.109	0.810 ± 0.210	0.866 ± 0.121	0.888 ± 0.095	0.891 ± 0.090
XGB (\uparrow)	0.851 ± 0.147	0.672 ± 0.307	0.814 ± 0.194	0.519 ± 0.897	0.802 ± 0.222	0.874 ± 0.125	0.874 ± 0.110	0.814 ± 0.209	0.870 ± 0.116	0.884 ± 0.102	0.886 ± 0.101
clf. (\uparrow)	0.907 ± 0.074	0.750 ± 0.227	0.895 ± 0.065	0.850 ± 0.114	0.868 ± 0.130	0.917 ± 0.064	0.913 ± 0.071	0.890 ± 0.081	0.918 ± 0.062	0.922 ± 0.063	0.922 ± 0.065
reg. (\uparrow)	0.586 ± 0.122	0.400 ± 0.266	0.472 ± 0.127	-0.641 ± 1.467	0.528 ± 0.239	0.660 ± 0.122	0.674 ± 0.095	0.506 ± 0.187	0.643 ± 0.061	0.698 ± 0.083	0.710 ± 0.092

4.2. Fidelity

Marginal density distribution of columns (Shape). TabTreeFormer achieves comparable performance to baseline models in “Shape” metric, as shown in Fig. 3. Meanwhile, it can be seen from Fig. 4 that TabTreeFormer captures better multimodal distribution compared to other auto-regressive transformers, which validates the effectiveness of our dual-quantization tokenizer design. More fidelity results can be found in Table 9 and Fig. 11 in Appendix D.1.

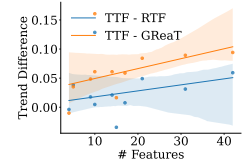
Pair-wise correlation between columns (Trend). TabTreeFormer outperforms all baselines in “Trend” metric with a significant margin, as presented in Fig. 3, implying the superior capability of TabTreeFormer in learning inter-feature relations. It can be observed from Fig. 5-6 that even strong baselines struggle with correlations involving cate-

gorical features and correlation values are not close to 0. Moreover, TabTreeFormer tends to show a more significant improvement from auto-regressive transformer baselines on datasets with a larger number of features as referred in Fig. 7. This also demonstrates the advantage of introducing the inductive bias to address *low-correlations* so that the models learn relations among a larger number of features better by filtering out less correlated features.

4.3. Utility (MLE)

The MLE results presented in Table 2 show that TabTreeFormer outperforms baseline models steadily regardless of the complexity of task, dataset, and ML model used. TTF-S achieves similar performance as the best-performing baselines (RTF and TabSyn), and TTF-M and TTF-L outperform them by a large margin of almost 40% in terms of relative

Figure 6. Real vs. synthetic abs. corr.



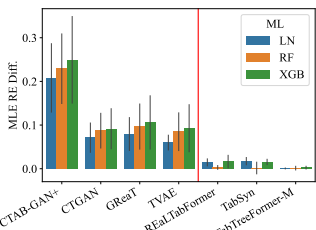


Figure 8. MLE relative error to real data with TabTreeFormer-L. On the left of the red line are rotationally invariant models.

Table 3. Privacy comparison of models. The first row shows the number of violations, and the second row shows the minimum p value for privacy leakage risk. The closer the value to 0, the higher the risk of privacy leakage. Risky values are highlighted in red.

	ARF	GReaT	RTF	TabSyn	TVAE	TTF-S	TTF-M	TTF-L
# vio.	0	5	0	0	1	1	0	0
min. p	0.071	0.000	0.097	0.141	0.003	0.045	0.061	0.111

errors in ML performance compared to real data. More MLE results can be found in Table 10 in Appendix D.2.

As an important foundation of tree-based models’ superior capability in capturing *potentially low-correlations, rotational invariance* of models is an aspect particularly worthwhile analyzing. As visualized in Fig. 8, rotationally invariant generators (e.g., CTAB-GAN+, CTGAN, GReaT, TVAE) are generally worse than non-rotationally invariant counterparts (e.g., REaLTabFormer and TabTreeFormer with a positional embedding in fixed order and TabSyn with VAE-encoding of data). Also, the advantage of TabTreeFormer over rotationally invariant baseline generators is more manifest on better-performing non-rotationally invariant downstream models (RF and XGB) than on rotationally invariant ones (LN). This again emphasizes the importance of applying non-rotationally invariant models to introduce inductive bias for *low correlations*.

4.4. Privacy (DCR)

As summarized in Table 3 TTF-M and TTF-L are privacy-resilient in all the 10 datasets. TabTreeFormer-S has a privacy leakage in only one dataset, with the p -value very close to 0.05. In comparison, GReaT demonstrates severe privacy concerns in 5 out of 10 datasets. Although auto-regressive transformers suffer from privacy leakage concerns, TabTreeFormer and REaLTabFormer are generally privacy-preserving, validating the effectiveness of token masking in protecting privacy for tabular auto-regressive transformers. Raw p -values per experiment are presented in Table 11 in Appendix D.3.

4.5. Efficiency

The efficiency of TabTreeFormer is mainly demonstrated by its ability to achieve better performance with a smaller model size. TTF-M surpasses all baselines in most metrics

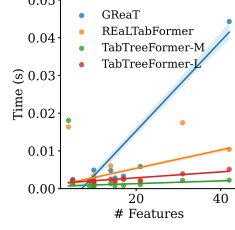


Figure 9. Number of features vs. average generation time per (valid) row.

Table 4. Relative performance change of TabTreeFormer-M compared to TabTreeFormer-L.

Fidelity		Utility	
Shape	-0.208%	Avg. MLE scores	-0.225%
Trend	-0.436%	Avg. MLE relative error	-9.624%

Table 5. Training time (s) comparison of TabTreeFormer and other auto-regressive transformer baselines on large datasets. The best values are highlighted in bold with an underscore, and the second best values are highlighted in bold without underscore.

Dataset	adult	bank	cahouse
GReaT	10397.040 ± 9.203	10295.769 ± 21.729	4373.950 ± 56.089
RTF	1875.904 ± 34.663	835.167 ± 1.619	596.523 ± 51.206
TTF-M	235.554 ± 71.542	225.707 ± 39.181	340.992 ± 76.571
TTF-L	606.790 ± 277.828	744.726 ± 221.487	946.903 ± 102.584

(i.e., fidelity, MLE, and DCR) as shown in Section 4.2-4.4. Notably, it only has approximately 5M parameters while the most competitive counterparts have more than 20M (TabSyn) or even more than 80M parameters (GReaT and REaLTabFormer). Also, as shown in Table 4, there is no significant performance gap between TTF-M and TTF-L, although their sizes differ eight times. This demonstrates the capability of TabTreeFormer in maintaining high efficiency without significant compromise in effectiveness.

Meanwhile, compared to baseline auto-regressive transformers, TabTreeFormer demonstrates a significant advantage in terms of training time on large datasets (see Table 5) and generation time on datasets with a large number of features (see Fig. 9), which is consistent with our expectation due to the smaller model size and sampling without rejection. Raw training and generation time records can be found in Table 13 in Appendix D.5.

4.6. Ablation Study

Table 6. Design component ablation. Relative score change when the corresponding component in TTF-S is taken out.

	LN	RF	XGB
w/o TBM	-4.121%	-4.798%	-7.657%
w/o DQT	-6.141%	-0.297%	-0.273%
w/o OCEL	+0.452%	-0.967%	-1.446%

We study the necessity of each building block in TabTreeFormer. It can be seen from Table 6 that TabTreeFormer experiences different degrees of noticeable performance degradation when we eliminate the tree-based model (TBM), dual-quantization tokenization (DQT), and OCEL, respectively, which verifies the indispensability of all building blocks. More results are presented in Appendix D.6.

5. Conclusion

In this paper, we propose TabTreeFormer, a hybrid tree-transformer for high-quality tabular data generation. TabTreeFormer inherits tabular-specific inductive biases from a tree-based model and captures multimodal distribution

for optimized numeric data representations via a dual-quantization tokenizer. We comprehensively evaluate the performance of TabTreeFormer and show that it demonstrates outstanding fidelity, utility, privacy, and efficiency with significantly smaller model sizes and computation time.

Acknowledgements

We would like to acknowledge Rishav Chourasia for helpful discussions.

References

Akiba, T., Sano, S., Yanase, T., Ohta, T., and Koyama, M. Optuna: A next-generation hyperparameter optimization framework. In Teredesai, A., Kumar, V., Li, Y., Rosales, R., Terzi, E., and Karypis, G. (eds.), *Proceedings of the 25th ACM SIGKDD International Conference on Knowledge Discovery & Data Mining, KDD 2019, Anchorage, AK, USA, August 4-8, 2019*, pp. 2623–2631. ACM, 2019. doi: 10.1145/3292500.3330701.

Arik, S. O. and Pfister, T. TabNet: Attentive interpretable tabular learning. *Proceedings of the AAAI Conference on Artificial Intelligence*, 35(8):6679–6687, May 2021. doi: 10.1609/aaai.v35i8.16826.

Assefa, S. A., Dervovic, D., Mahfouz, M., Tillman, R. E., Reddy, P., and Veloso, M. Generating synthetic data in finance: opportunities, challenges and pitfalls. In *Proceedings of the First ACM International Conference on AI in Finance, ICAIF '20*, New York, NY, USA, 2021. Association for Computing Machinery. ISBN 9781450375849. doi: 10.1145/3383455.3422554.

Bishop, C. M. *Pattern Recognition and Machine Learning (Information Science and Statistics)*. Springer-Verlag, Berlin, Heidelberg, 2006. ISBN 0387310738.

Borisov, V., Sessler, K., Leemann, T., Pawelczyk, M., and Kasneci, G. Language models are realistic tabular data generators. In *The Eleventh International Conference on Learning Representations*, 2023.

Breiman, L. Random forests. *Machine learning*, 45(1):5–32, 2001. ISSN 1573-0565. doi: 10.1023/A:1010933404324.

Chen, T. and Guestrin, C. XGBoost: A scalable tree boosting system. In Krishnapuram, B., Shah, M., Smola, A. J., Aggarwal, C. C., Shen, D., and Rastogi, R. (eds.), *Proceedings of the 22nd ACM SIGKDD International Conference on Knowledge Discovery and Data Mining, San Francisco, CA, USA, August 13-17, 2016*, pp. 785–794. ACM, 2016. doi: 10.1145/2939672.2939785.

Dai, Z., Yang, Z., Yang, Y., Carbonell, J. G., Le, Q. V., and Salakhutdinov, R. Transformer-xl: Attentive language models beyond a fixed-length context. In Korhonen, A., Traum, D. R., and Márquez, L. (eds.), *Proceedings of the 57th Conference of the Association for Computational Linguistics, ACL 2019, Florence, Italy, July 28-August 2, 2019, Volume 1: Long Papers*, pp. 2978–2988. Association for Computational Linguistics, 2019. doi: 10.18653/V1/P19-1285.

Dash, S., Shakyawar, S. K., Sharma, M., and Kaushik, S. Big data in healthcare: management, analysis and future prospects. *Journal of Big Data*, 6(1):54, 2019. ISSN 2196-1115. doi: 10.1186/s40537-019-0217-0.

Synthetic Data Metrics. DataCebo, Inc., 12 2023. URL <https://docs.sdv.dev/sdmetrics/>. Version 0.13.0.

Dosovitskiy, A., Beyer, L., Kolesnikov, A., Weissenborn, D., Zhai, X., Unterthiner, T., Dehghani, M., Minderer, M., Heigold, G., Gelly, S., Uszkoreit, J., and Houlsby, N. An image is worth 16x16 words: Transformers for image recognition at scale. In *9th International Conference on Learning Representations, ICLR 2021, Virtual Event, Austria, May 3-7, 2021*. OpenReview.net, 2021.

EU. Regulation (EU) 2016/679 of the European parliament and of the council of 27 April 2016 on the protection of natural persons with regard to the processing of personal data and on the free movement of such data, and repealing directive 95/46/EC (General Data Protection Regulation). *OJ*, L 119, Apr 2016. URL <https://gdpr-info.eu/>.

Fisher, R. A. The use of multiple measurements in taxonomic problems. *Annals of Eugenics*, 7(2):179–188, Sep 1936. doi: 10.1111/j.1469-1809.1936.tb02137.x.

Gorishniy, Y., Rubachev, I., Khrulkov, V., and Babenko, A. Revisiting deep learning models for tabular data. In Ranzato, M., Beygelzimer, A., Dauphin, Y., Liang, P., and Vaughan, J. W. (eds.), *Advances in Neural Information Processing Systems*, volume 34, pp. 18932–18943, Red Hook, NY, USA, 2021. Curran Associates, Inc. ISBN 9781713845393.

Grinsztajn, L., Oyallon, E., and Varoquaux, G. Why do tree-based models still outperform deep learning on typical tabular data? In Koyejo, S., Mohamed, S., Agarwal, A., Belgrave, D., Cho, K., and Oh, A. (eds.), *Advances in Neural Information Processing Systems*, volume 35, pp. 507–520, Red Hook, NY, USA, 2022. Curran Associates, Inc. ISBN 9781713871088.

Gulati, M. and Roysdon, P. TabMT: Generating tabular data with masked transformers. In Oh, A., Naumann, T., Globerson, A., Saenko, K., Hardt, M., and Levine, S. (eds.), *Advances in Neural Information Processing*

Systems, volume 36, pp. 46245–46254, Red Hook, NY, USA, 2023. Curran Associates, Inc.

Harrison, D. and Rubinfeld, D. L. Hedonic housing prices and the demand for clean air. *JEEM*, 5(1):81–102, 1978. ISSN 0095-0696.

Hernandez, M., Epelde, G., Alberdi, A., Cilla, R., and Rankin, D. Synthetic data generation for tabular health records: A systematic review. *Neurocomputing*, 493:28–45, 2022. ISSN 0925-2312. doi: <https://doi.org/10.1016/j.neucom.2022.04.053>.

Hofmann, H. Statlog (German Credit Data). UCI Machine Learning Repository, 1994. DOI: <https://doi.org/10.24432/C5NC77>.

Hollmann, N., Müller, S., Eggensperger, K., and Hutter, F. TabPFN: A transformer that solves small tabular classification problems in a second. In *The Eleventh International Conference on Learning Representations, ICLR 2023, Kigali, Rwanda, May 1-5, 2023*. OpenReview.net, 2023.

Huang, X., Khetan, A., Cvitkovic, M., and Karnin, Z. TabTransformer: Tabular data modeling using contextual embeddings, 2020. URL <https://arxiv.org/abs/2012.06678>.

Ke, G., Meng, Q., Finley, T., Wang, T., Chen, W., Ma, W., Ye, Q., and Liu, T.-Y. LightGBM: A highly efficient gradient boosting decision tree. In Guyon, I., Luxburg, U. V., Bengio, S., Wallach, H., Fergus, R., Vishwanathan, S., and Garnett, R. (eds.), *Advances in Neural Information Processing Systems*, volume 30, Red Hook, NY, USA, 2017. Curran Associates, Inc. ISBN 9781510860964.

Kelley Pace, R. and Barry, R. Sparse spatial autoregressions. *Statistics & Probability Letters*, 33(3):291–297, 1997. ISSN 0167-7152.

Kohavi, R. Scaling up the accuracy of Naive-Bayes classifiers: a decision-tree hybrid. In *Proceedings of the Second International Conference on Knowledge Discovery and Data Mining, KDD’96*, pp. 202–207. AAAI Press, 1996.

Kotelnikov, A., Baranchuk, D., Rubachev, I., and Babenko, A. TabDDPM: Modelling tabular data with diffusion models. In Krause, A., Brunskill, E., Cho, K., Engelhardt, B., Sabato, S., and Scarlett, J. (eds.), *Proceedings of the 40th International Conference on Machine Learning*, volume 202 of *Proceedings of Machine Learning Research*, pp. 17564–17579. PMLR, 23–29 Jul 2023.

MacQueen, J. Some methods for classification and analysis of multivariate observations. In Le Cam, L. M. and Neyman, J. (eds.), *Proceedings of the Fifth Berkeley Symposium on Mathematical Statistics and Probability*, volume 1, pp. 281–297. University of California Press, Berkeley, CA, 1967.

Mann, H. B. and Whitney, D. R. On a test of whether one of two random variables is stochastically larger than the other. *The Annals of Mathematical Statistics*, 18(1):50–60, 1947. doi: 10.1214/aoms/1177730491.

Mansouri, K., Ringsted, T., Ballabio, D., Todeschini, R., and Consonni, V. Quantitative structure–activity relationship models for ready biodegradability of chemicals. *Journal of Chemical Information and Modeling*, 53(4):867–878, 2013. doi: 10.1021/ci4000213. PMID: 23469921.

McCarter, C. Unmasking trees for tabular data, 2024. URL <https://arxiv.org/abs/2407.05593>.

Moro, S., Cortez, P., and Laureano, R. Using data mining for bank direct marketing: An application of the CRISP-DM methodology. In *Proceedings of the European Simulation and Modelling Conference*, 10 2011.

Ng, A. Y. Feature selection, L1 vs. L2 regularization, and rotational invariance. In *Proceedings of the Twenty-First International Conference on Machine Learning, ICML ’04*, pp. 78, New York, NY, USA, 2004. Association for Computing Machinery. ISBN 1581138385. doi: 10.1145/1015330.1015435.

Park, N., Mohammadi, M., Gorde, K., Jajodia, S., Park, H., and Kim, Y. Data synthesis based on generative adversarial networks. *Proc. VLDB Endow.*, 11(10):1071–1083, Jun 2018. ISSN 2150-8097. doi: 10.14778/3231751.3231757.

PDPC. Proposed guide on synthetic data generation. *Personal Data Protection Commission*, July 2024. URL <https://www.pdpc.gov.sg/help-and-resources/2024/07/proposed-guide-on-synthetic-data-generation>. Accessed: 2024-12-26.

Prokhorenkova, L., Gusev, G., Vorobev, A., Dorogush, A. V., and Gulin, A. CatBoost: unbiased boosting with categorical features. In Bengio, S., Wallach, H., Larochelle, H., Grauman, K., Cesa-Bianchi, N., and Garnett, R. (eds.), *Advances in Neural Information Processing Systems*, volume 31, pp. 6639–6649, Red Hook, NY, USA, 2018. Curran Associates, Inc.

Qian, Z., Davis, R., and van der Schaar, M. Synthcity: a benchmark framework for diverse use cases of tabular synthetic data. In Oh, A., Naumann, T., Globerson, A., Saenko, K., Hardt, M., and Levine, S. (eds.), *Advances in Neural Information Processing Systems*, volume 36, pp. 3173–3188, Red Hook, NY, USA, 2023. Curran Associates, Inc.

Radford, A., Wu, J., Child, R., Luan, D., Amodei, D., and Sutskever, I. Language models are unsupervised multitask learners. *OpenAI Blog*, 1(8), 2019. URL https://cdn.openai.com/better-language-models/language_models_are_unsupervised_multitask_learners.pdf.

Rahaman, N., Baratin, A., Arpit, D., Draxler, F., Lin, M., Hamprecht, F. A., Bengio, Y., and Courville, A. C. On the spectral bias of neural networks. In Chaudhuri, K. and Salakhutdinov, R. (eds.), *Proceedings of the 36th International Conference on Machine Learning*, volume 97 of *Proceedings of Machine Learning Research*, pp. 5301–5310. PMLR, 09–15 Jun 2019.

Sanh, V., Debut, L., Chaumond, J., and Wolf, T. DistilBERT, a distilled version of BERT: smaller, faster, cheaper and lighter. In *NeurIPS EMC2 Workshop*, 2019.

Shi, J., Xu, M., Hua, H., Zhang, H., Ermon, S., and Leskovec, J. TabDiff: a multi-modal diffusion model for tabular data generation, 2024. URL <https://arxiv.org/abs/2410.20626>.

Shwartz-Ziv, R. and Armon, A. Tabular data: Deep learning is not all you need. *Inf. Fusion*, 81(C):84–90, May 2022. ISSN 1566-2535. doi: 10.1016/j.inffus.2021.11.011.

Smith, J., Everhart, J., Dickson, W., Knowler, W., and Johannes, R. Using the ADAP learning algorithm to forecast the onset of diabetes mellitus. *Proc. Annu. Symp. Comput. Appl. Med. Care*, 10, 11 1988.

Solatorio, A. V. and Dupriez, O. REaLTabFormer: Generating realistic relational and tabular data using transformers, 2023. URL <https://arxiv.org/abs/2302.02041>.

Street, W. N., Wolberg, W. H., and Mangasarian, O. L. Nuclear feature extraction for breast tumor diagnosis. In Acharya, R. S. and Goldgof, D. B. (eds.), *Biomedical Image Processing and Biomedical Visualization*, volume 1905, pp. 861 – 870. International Society for Optics and Photonics, SPIE, 1993.

Vanschoren, J., van Rijn, J. N., Bischl, B., and Torgo, L. OpenML: Networked science in machine learning. *SIGKDD Explorations*, 15(2):49–60, 2013. doi: 10.1145/2641190.2641198.

Vaswani, A., Shazeer, N., Parmar, N., Uszkoreit, J., Jones, L., Gomez, A. N., Kaiser, L. u., and Polosukhin, I. Attention is all you need. In Guyon, I., Luxburg, U. V., Bengio, S., Wallach, H., Fergus, R., Vishwanathan, S., and Garnett, R. (eds.), *Advances in Neural Information Processing Systems*, volume 30, pp. 6000–6010, Red Hook, NY, USA, 2017. Curran Associates, Inc. ISBN 9781510860964.

Watson, D. S., Blesch, K., Kapar, J., and Wright, M. N. Adversarial random forests for density estimation and generative modeling. In Ruiz, F., Dy, J., and van de Meent, J.-W. (eds.), *Proceedings of The 26th International Conference on Artificial Intelligence and Statistics*, volume 206 of *Proceedings of Machine Learning Research*, pp. 5357–5375. PMLR, 25–27 Apr 2023.

Wolberg, W. H. and Mangasarian, O. L. Multisurface method of pattern separation for medical diagnosis applied to breast cytology. *PNAS*, 87(23):9193–9196, 1990.

Wu, H., Xiao, B., Codella, N., Liu, M., Dai, X., Yuan, L., and Zhang, L. CvT: Introducing convolutions to vision transformers. In *2021 IEEE/CVF International Conference on Computer Vision (ICCV)*, pp. 22–31, 2021. doi: 10.1109/ICCV48922.2021.00009.

Xu, L., Skouliaridou, M., Cuesta-Infante, A., and Veeramachaneni, K. Modeling tabular data using conditional GAN. In Wallach, H., Larochelle, H., Beygelzimer, A., d'Alché-Buc, F., Fox, E., and Garnett, R. (eds.), *Advances in Neural Information Processing Systems*, volume 32, pp. 7335–7345, Red Hook, NY, USA, 2019. Curran Associates, Inc.

Zhang, H., Zhang, J., Shen, Z., Srinivasan, B., Qin, X., Faloutsos, C., Rangwala, H., and Karypis, G. Mixed-type tabular data synthesis with score-based diffusion in latent space. In *The Twelfth International Conference on Learning Representations, ICLR 2024, Vienna, Austria, May 7-11, 2024*. OpenReview.net, 2024.

Zhao, Z., Kunar, A., Birke, R., and Chen, L. Y. CTAB-GAN: Effective table data synthesizing. In Balasubramanian, V. N. and Tsang, I. (eds.), *Proceedings of The 13th Asian Conference on Machine Learning*, volume 157 of *Proceedings of Machine Learning Research*, pp. 97–112. PMLR, 17–19 Nov 2021.

Zhao, Z., Birke, R., and Chen, L. TabuLa: Harnessing language models for tabular data synthesis, 2023. URL <https://arxiv.org/abs/2310.12746>.

Zhao, Z., Kunar, A., Birke, R., Van der Scheer, H., and Chen, L. Y. CTAB-GAN+: enhancing tabular data synthesis. *Frontiers in Big Data*, 6, 2024. ISSN 2624-909X. doi: 10.3389/fdata.2023.1296508.

A. Supplementary Loss Function Explanation and Analysis

A.1. Proof of Lemma 1

Proof. Firstly, note that $\frac{\partial w_{ti}}{\partial z_j} = 0, \forall i, j \in \{1, \dots, V\}$, by independence between the two. Also mind that $w_{ti} > 0, \forall i \in \{1, \dots, V\}$.

$$\begin{aligned}
 & \frac{\partial \mathcal{L}_{\text{oce}}(\mathbf{z}, t)}{\partial z_t} \\
 &= - \frac{\sum_{i=1}^V w_{ti} e^{z_i}}{w_{tt} e^{z_t}} \cdot \frac{w_{tt} e^{z_t} \sum_{i=1}^V w_{ti} e^{z_i} - w_{tt} e^{z_t} \cdot w_{tt} e^{z_t}}{\left(\sum_{i=1}^V w_{ti} e^{z_i}\right)^2} \\
 &= - \frac{\sum_{i=1}^V w_{ti} e^{z_i} - w_{tt} e^{z_t}}{\sum_{i=1}^V w_{ti} e^{z_i}} < 0 \\
 & \frac{\partial \mathcal{L}_{\text{oce}}(\mathbf{z}, t)}{\partial z_i} \\
 &= - \frac{\sum_{i=1}^V w_{ti} e^{z_i}}{w_{tt} e^{z_t}} \cdot \frac{-w_{ti} e^{z_i} \cdot w_{tt} e^{z_t}}{\left(\sum_{i=1}^V w_{ti} e^{z_i}\right)^2} \\
 &= \frac{w_{ti} e^{z_i}}{\sum_{i=1}^V w_{ti} e^{z_i}} > 0
 \end{aligned}$$

Thus, $\mathcal{L}_{\text{oce}}(\mathbf{z}, t)$ is optimized (minimized) when $z_t \rightarrow \infty, z_i \rightarrow -\infty (i \neq t)$. \square

A.2. Proof of Theorem 1

Proof. Express \mathcal{L}_{oce} and \mathcal{L}_{ce} using \mathbf{p} , we have

$$\mathcal{L}_{\text{ce}}(\mathbf{z}, t) = -\log p_t \quad (6)$$

$$\begin{aligned}
 \mathcal{L}_{\text{oce}}(\mathbf{z}, t) &= -\log \frac{w_{tt} e^{z_t}}{\sum_{i=1}^V w_{ti} e^{z_i}} \\
 &= -\log \frac{w_{tt} \cdot \frac{e^{z_t}}{\sum_{i=1}^V e^{z_i}}}{\sum_{i=1}^V w_{ti} \cdot \frac{e^{z_i}}{\sum_{j=1}^V e^{z_j}}} \\
 &= -\log \frac{w_{tt} p_t}{\sum_{i=1}^V w_{ti} p_i} \\
 &= -\log \frac{w_{tt} p_t}{D(\mathbf{z})} \quad (7)
 \end{aligned}$$

By $\mathcal{L}_{\text{ce}}(\mathbf{z}, t) = \mathcal{L}_{\text{ce}}(\mathbf{z}^*, t)$, we have $p_t = p_t^*$. Given $D(\mathbf{z}) < D(\mathbf{z}^*)$, we must have $\mathcal{L}_{\text{oce}}(\mathbf{z}, t) < \mathcal{L}_{\text{oce}}(\mathbf{z}^*, t)$. \square

A.3. Detailed Explanations and Analysis of the Weight Function (Equation 3)

Recall the function of weight given the target token and current token in Equation 3. This section will provide detailed explanations and analysis of it.

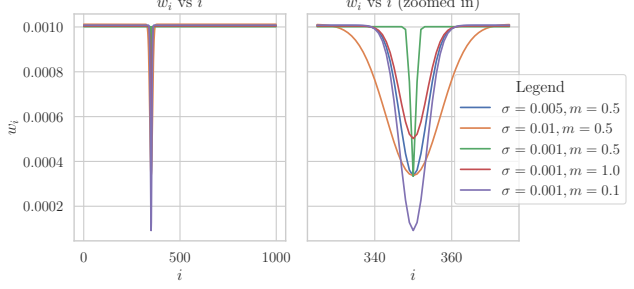


Figure 10. The relation of weights w_{ti} (normalized so that $\|\mathbf{w}\| = 1$ for visualization purpose to token index i , with vocabulary size $V = 1000$, and target token $t = 350$.

The exponential term comes from the intuition that the difference between closer quantiles is much more significant than the difference between farther quantiles. Some scaling and shifting is applied on the exponential term.

Figure 10 illustrates the relationship between w_{ti} and i under varying values of σ and m . The parameter σ primarily governs the width around the target token where the weights are significantly altered; larger σ values result in a broader width. In contrast, m dictates the intensity of the weight modification, with smaller m values leading to more pronounced changes in weight.

B. TabTreeFormer Model Setup Details

B.1. Tree-based Model

B.1.1. HYPERPARAMETER TUNING

For the tree-based classifier or regressor, we use Optuna (Akiba et al., 2019) to tune the hyperparameters of LightGBM (Ke et al., 2017) using the training data. If the dataset has a designated target column, the model is trained to predict that column. Otherwise, a random column can be selected as the target. Then, fit the model with the selected hyperparameters for TabTreeFormer.

The hyperparameter space explored is

- Learning Rate:** Logarithmic scale float in $[0.01, 0.3]$;
- Number of Estimators:** Integers in $[50, 250]$ step 50;
- Maximum Depth:** Integers in $[3, 10]$;
- Number of Leaves:** Integers in $[20, 100]$ step 5;
- Minimum Size per Leaf:** Integers in $[10, 50]$ step 5;
- Feature Fraction:** Float in $[0.6, 1.0]$;
- Bagging Fraction:** Float in $[0.6, 1.0]$;
- L1 Regularization:** Float in $[0.0, 10.0]$;
- L2 Regularization:** Float in $[0.0, 10.0]$.

Optimization was performed over 50 trials using 3-fold cross-validation, performance evaluated based on weighted F1 for classification and (negative) mean squared error for regression.

B.1.2. LEAF INDEX MATRIX

In the subsequent steps of TabTreeFormer, *leaf index matrix* \mathbf{J} of the real data \mathbf{X} is computed. The indexing order of trees and their leaves used in the subsequent steps are directly taken from the fitted tree-based model. The *leaf index matrix* is essentially the result of `.apply` function for most tree-based models in `sklearn`.

B.2. Tokenization

For K-Means and quantile quantization, we use `sklearn.preprocessing.KBinsDiscretizer` with strategy “kmeans” and “quantile” respectively.

In cases where the number of distinct values expected to be kept is way larger than typical natural language models’ vocabulary size, two or more consecutive quantile quantizers may be used, where subsequent quantizers are used to quantize the values in the same quantile as suggested by previous quantizers. Thus, with q quantizers, a total of Q^q values can be represented, which is sufficient to cover most practical cases. In this paper, we present $Q = 1000$ as sufficient precision for simplicity.

For categorical values, we use `sklearn.preprocessing.OrdinalEncoder`.

B.3. Transformer

B.3.1. MODEL CONFIGURATION

For the language model, we use Distill-GPT2 (Sanh et al., 2019), based on the GPT architecture (Radford et al., 2019), with several modifications. The vocabulary size and maximum sequence length are adjusted based on the dataset, and the values are likely much lower than the requirement for natural language models. For example, if $n_l = 200, n_c = 20, n_b = K = 10, n_q = Q = 1000$, then $V = 1233$, and if $T = 200, m_d = 10, m_c = 10$, then $L = 222$, while natural language models typically have $V > 30000, L > 1000$.

In this paper, we present 3 versions of TabTreeFormer of different sizes. Table 7 shows their details. The model sizes are obtained for diabetes (Smith et al., 1988) dataset. Actual values may vary based on the fitted tree-based model and dataset.

Table 7. Hyperparameter configuration of TabTreeFormer of different sizes.

TabTreeFormer	S	M	L
Approx. #Params (in M)	1	5	40
hidden state dimensions	128	256	768
inner feed-forwarded layer dimensions	256	1024	3072
number of attention heads per layer	8	8	12

B.3.2. TOKEN SEQUENCE CONSTRUCTION

The tokens in Table 1 are conceptual tokens. When converting the leaf, category, K-Means bin, and quantile IDs into token IDs in actual implementation, we do not explicitly make the textual tokens, but instead, directly add corresponding token type’s offset.

B.3.3. MASKING

Instead of using a fixed mask ratio, we apply varying mask ratios to enhance the diversity of training data. Tree-related tokens (yellow section in Figure 2) are masked with a ratio sampled uniformly from $[0.3, 0.7]$, while actual value tokens (blue section in Figure 2) are masked with a ratio sampled uniformly from $[0.1, 0.4]$.

To ensure that the quantile token is always masked if its corresponding K-Means bin token is masked within the same numeric column, we first generate a random mask. If a violation is detected (i.e., the K-Means bin token is unmasked while the quantile token is masked), we swap the mask values of these two positions. This approach ensures that masks are generated both efficiently and accurately.

B.3.4. TRAINING CONFIGURATION

The reduced model size allows for a significantly larger batch size compared to typical natural language models. We use a batch size of 128 per device, reduce by half in case of CUDA OOM¹, and train for up to 3,000 steps with a learning rate of 5×10^{-4} in FP16 precision, utilizing the Hugging Face Trainer.

B.3.5. MODEL INFERENCE

Tree-leaf tokens from real data after masking are used as prompts for generation. We apply a temperature of 0.7 with sampling for generation.

Recall that a set of valid tokens can be pre-determined at each position. Formally, let p_i be the corresponding feature index for the i -th token from data tokenizer, and R_i indicates the type of this token. For example, in Figure 2, $p_1 = 1, p_2 = 1, p_3 = 2, R_1 = \text{bin}, R_2 = \text{quant}, R_3 = \text{cat}$. Then, let \mathcal{V}_i be the set of tokens allowed at position $i \in \{1, 2, \dots, L\}$ in the entire sequence, we have Equation 8.

$$\mathcal{V}_i = \begin{cases} \{\text{[BOS]}\} & \text{if } i = 1 \\ \{\text{[leaf1]}, \dots, \text{[leaf}(l_{i-1})\}\} & \text{if } 2 \leq i \leq T + 1 \\ \{\text{[bin1]}, \dots, \text{[bin}(b_{p_{i-T-1}})\}\} & \text{if } T + 2 \leq i \leq L - 1 \text{ and } R_{i-T-1} = \text{bin} \\ \{\text{[quant1]}, \dots, \text{[quant}(q_{p_{i-T-1}})\}\} & \text{if } T + 2 \leq i \leq L - 1 \text{ and } R_{i-T-1} = \text{quant} \\ \{\text{[cat1]}, \dots, \text{[cat}(b_{p_{i-T-1}})\}\} & \text{if } T + 2 \leq i \leq L - 1 \text{ and } R_{i-T-1} = \text{cat} \\ \{\text{[EOS]}\} & \text{if } i = L \end{cases} \quad (8)$$

¹Among all $10 \times 3 = 30$ experiments, TabTreeFormer-L hits CUDA OOM in one experiment, and no other TabTreeFormer experiments had memory issues with this batch size.

Valid tokens for a specific position is enforced by setting the logits of invalid tokens at the position to negative infinity before sampling.

C. Experiment Setup Details

C.1. Experiment Environment

Experiments were conducted on a system running Ubuntu 22.04.1 LTS with kernel version 6.8.0. The machine featured a 13th Gen Intel Core i9-13900K CPU with 24 cores and 32 threads, capable of a maximum clock speed of 5.8 GHz. GPU computations were performed using a single NVIDIA GeForce RTX 4090 with 24 GB VRAM. The environment was set up with NVIDIA driver version 565.57.01 and CUDA 12.7.

C.2. Details on Datasets

Table 8 shows the details of the datasets we used. Datasets are downloaded by `sklearn.datasets.fetch_openml`, with the dataset name as input.

C.3. Baseline Implementation

We use the Synthcity (Qian et al., 2023) implementation for ARF (Watson et al., 2023), CTGAN (Xu et al., 2019), GReaT (Borisov et al., 2023), TabDDPM (Kotelnikov et al., 2023), and TVAE (Xu et al., 2019). We also include CTABGAN+ (Zhao et al., 2024), REaLTabFormer (Solatorio & Dupriez, 2023), and TabSyn (Zhang et al., 2024) using their official code on GitHub or public SDK.

C.4. Fidelity Metrics Implementation

Fidelity metrics are calculated using SDMetrics (Dat, 2023)'s public SDK.

C.5. Machine Learning Efficacy (MLE) Metrics Implementation

Instead of running all models with fixed, typically default, parameters across all datasets, we perform hyperparameter tuning before reporting their performance. The tuning process follows the same methodology used to optimize the core tree-based model in TabTreeFormer, but with 30 trials per round of optimization.

For linear models, no hyperparameter tuning is performed, as they follow the classical definition without additional tunable parameters.

The hyperparameter space explored for random forest is

- **Number of Estimators:** Integers in [100, 300] step 50;
- **Maximum Depth:** Integers in [5, 20] step 5;

- **Minimum Samples Split:** Integers in [2, 10] step 2;
- **Minimum Size per Leaf:** Integers [1, 5];
- **Maximum Features:** Value in “sqrt”, “log2”, and NULL;
- **Bootstramp:** Enabled or disabled.

The hyperparameter space explored for XGBoost is:

- **Learning Rate:** Logarithmic scale float in [0.01, 0.3];
- **Number of Estimators:** Integers in [100, 300] step 50;
- **Maximum Depth:** Integers in [3, 10];
- **Minimum Child Weight:** Logarithmic scale float in [1.0, 10.0];
- **Minimum Split Loss Gamma:** Float in [0.0, 0.5];
- **Subsample Ratio:** Float in [0.5, 1.0];
- **Subsample Ratio of Columns by Tree:** Float in [0.5, 1.0];
- **L1 Regularization:** Float in [0.0, 10.0].

For all models, numeric values are standardized using standard scaling. Categorical values are one-hot encoded for linear models and label-encoded for random forest and XGBoost. To simplify the experiments, rows with missing values are excluded, as handling missing data is not the focus of this paper.

The reported performance for machine learning utility is measured using the weighted AUC-ROC for classification tasks and the R^2 score for regression tasks, so for all these scores, a larger value indicates a better performance. Each generator is trained and used to generate synthetic data of the same size as the training dataset three times for each dataset, and the summarized results of these runs are reported.

C.6. Distance to Closest Record (DCR) Metrics Implementation

The way the DCR values are reported differ from paper to paper. Also, existing papers often report a value and claim some specific value to be an ideal value, overlooking the fact that better privacy usually sacrifices quality. Thus, in this paper, we instead apply a statistical test on DCR values to validate privacy-preserving capability of the models, instead of evaluating it, which is likely also more useful in practical privacy-preserving data sharing cases.

We compare the DCR to the real training dataset \mathbf{X} of a hold-out real dataset $\widehat{\mathbf{X}}$ with a synthetic dataset of the same size \mathbf{X}' , and privacy-preserving means that DCRs calculated on the latter is not smaller than DCRs calculated on the former. We test this using Mann-Whitney U Test (Mann & Whitney, 1947), with the null hypothesis H_0 being that the distance between $\widehat{\mathbf{X}}$ and \mathbf{X} is greater than or equal to \mathbf{X}' and \mathbf{X} , and if the p -value is less than 0.05, \mathbf{X}' is closer to \mathbf{X} than $\widehat{\mathbf{X}}$, implying a risk of privacy leakage.

The data is preprocessed by standard scaling for numeric val-

Table 8. Datasets used in experiments. #R, #F, #N, and #C represents the number of rows, features (including target column), numeric features, and categorical features respectively. The task can be classification, denoted “clf” followed by the number of classes in the bracket, and regression, denoted “reg”. Aliases in bracket in “Name” column show the names used in this paper.

Name	#R	#F	#N	#C	Task
adult (Kohavi, 1996)	48842	15	2	13	clf(2)
bank-marketing (bank) (Moro et al., 2011)	45211	17	7	10	clf(2)
boston (Harrison & Rubinfeld, 1978)	506	14	12	2	reg
breast-w (breast) (Wolberg & Mangasarian, 1990)	699	10	9	1	clf(2)
california_housing (cahouse) (Kelley Pace & Barry, 1997)	20640	10	9	1	reg
credit-g (credit) (Hofmann, 1994)	1000	21	7	14	clf(2)
diabetes (Smith et al., 1988)	768	9	8	1	clf(2)
iris (Fisher, 1936)	150	5	4	1	clf(3)
qsar-biodeg (qsar) (Mansouri et al., 2013)	1055	42	41	1	clf(2)
wdbc (Street et al., 1993)	569	31	30	1	clf(2)

ues and one-hot encoding for categorical values for distance calculation. Cosine distance (calculated using `sklearn`) is used to evaluate the distance between records. As a reference, we calculate the cosine distances between the real test set and the real train set, obtaining the minimum distance per record for the test set. Similarly, we compute the cosine distances between synthetic data (with the same number of rows as the real test set) and the real train set, and also obtain the minimum distances. These distances are compared with the reference values to assess the similarity and privacy-preserving characteristics of the synthetic data.

C.7. Real Data Detection (RDD) Metrics Implementation

This metric is not discussed in the main paper as it does not directly pertain to the primary use cases of synthetic data. However, since it is a standard evaluation framework, we include it in the appendix for completeness.

The RDD metric evaluates how easily real data can be distinguished from synthetic data. A higher difficulty in detection indicates better synthetic data quality. The evaluation is framed as a binary classification task, with the experimental settings kept the same as those used for machine learning efficacy (MLE). However, unlike MLE, where higher scores are better, for RDD, lower AUC-ROC values indicate better performance, as they reflect greater similarity between synthetic and real data.

The training data for the RDD task consists of the real training set combined with a synthetic dataset of the same size as the real training set. The test data comprises the real test set combined with another synthetic dataset of the same size as the real test set.

D. Supplementary Experimental Results

D.1. Supplementary Fidelity Results

The raw experiment results for fidelity is shown in Table 9.

Figure 11 shows the performance of TabTreeFormer in comparison to other auto-regressive transformers in capturing multimodal distributions. TabTreeFormer shows a better capability in capturing such distribution in general.

D.2. Supplementary Utility Results

The raw experiment results for MLE is shown in Table 10. The results are also visualized in Figure 12. Out of the 30 MLE scores, TabTreeFormer-M or -L outperforms all other baselines in 20 cases (2/3), and they both outperform all other baselines in 16 cases ($\geq 1/2$).

D.3. Supplementary Privacy Results

The raw experiment results for DCR is shown in Table 11.

D.4. RDD Evaluation Results

Table 12 shows the result for RDD. Since TabTreeFormernaïvely use mean value as the reverse quantization step, it is expected that as long as a detector is able to detect these specific recovered quantized values, TabTreeFormer-generated records can be detected. Even so, TabTreeFormer still outperforms all baselines except for REaLTabFormer (Solatorio & Dupriez, 2023).

D.5. Computation Time

TabTreeFormer is trained by limiting the total number of training steps instead of the number of epochs, so the training time of it on smaller datasets are usually longer.

Table 9. Performance comparison between different models in terms of fidelity. The closer the values are to 1, the better the fidelity is. The best scores and the second best scores are highlighted in bold with and without underscore, respectively. Equal values in the first 3 digits may be compared by the 4-th or 5-th digits.

Dataset	Metric	ARF	CTAB+	CTGAN	TabDDPM	GReaT	RTF	TabSyn	TVAE	TTF-S	TTF-M	TTF-L
adult	Shape	0.942 \pm 0.001	0.964 \pm 0.005	0.881 \pm 0.008	0.983 \pm 0.001	0.929 \pm 0.006	0.962 \pm 0.001	0.977 \pm 0.011	0.877 \pm 0.004	0.946 \pm 0.002	0.954 \pm 0.001	0.956 \pm 0.001
	Trend	0.876 \pm 0.004	0.915 \pm 0.004	0.760 \pm 0.005	0.953 \pm 0.006	0.882 \pm 0.000	0.933 \pm 0.003	0.955 \pm 0.018	0.726 \pm 0.002	0.869 \pm 0.017	0.883 \pm 0.020	0.899 \pm 0.001
bank	Shape	0.947 \pm 0.000	0.965 \pm 0.002	0.891 \pm 0.001	0.983 \pm 0.001	0.915 \pm 0.000	0.967 \pm 0.001	0.983 \pm 0.005	0.894 \pm 0.003	0.906 \pm 0.006	0.929 \pm 0.001	0.937 \pm 0.001
	Trend	0.885 \pm 0.019	0.884 \pm 0.003	0.870 \pm 0.009	0.932 \pm 0.030	0.903 \pm 0.000	0.955 \pm 0.001	0.967 \pm 0.008	0.870 \pm 0.011	0.925 \pm 0.011	0.954 \pm 0.001	0.962 \pm 0.002
boston	Shape	0.907 \pm 0.005	0.850 \pm 0.003	0.795 \pm 0.023	0.489 \pm 0.025	0.916 \pm 0.000	0.942 \pm 0.004	0.893 \pm 0.003	0.801 \pm 0.009	0.850 \pm 0.001	0.855 \pm 0.000	0.856 \pm 0.001
	Trend	0.921 \pm 0.005	0.828 \pm 0.011	0.896 \pm 0.004	0.606 \pm 0.006	0.908 \pm 0.000	0.947 \pm 0.002	0.934 \pm 0.003	0.843 \pm 0.005	0.944 \pm 0.003	0.968 \pm 0.001	0.969 \pm 0.000
breast	Shape	0.854 \pm 0.005	0.775 \pm 0.024	0.832 \pm 0.019	0.838 \pm 0.001	0.728 \pm 0.000	0.753 \pm 0.014	0.813 \pm 0.005	0.900 \pm 0.013	0.820 \pm 0.011	0.851 \pm 0.002	0.852 \pm 0.008
	Trend	0.767 \pm 0.006	0.616 \pm 0.063	0.709 \pm 0.015	0.767 \pm 0.000	0.636 \pm 0.000	0.668 \pm 0.010	0.709 \pm 0.006	0.781 \pm 0.010	0.749 \pm 0.010	0.799 \pm 0.003	0.796 \pm 0.016
cahouse	Shape	0.979 \pm 0.001	0.962 \pm 0.003	0.908 \pm 0.005	0.974 \pm 0.006	0.879 \pm 0.000	0.974 \pm 0.003	0.991 \pm 0.001	0.944 \pm 0.001	0.949 \pm 0.006	0.975 \pm 0.001	0.979 \pm 0.000
	Trend	0.971 \pm 0.002	0.927 \pm 0.002	0.914 \pm 0.004	0.946 \pm 0.002	0.913 \pm 0.000	0.969 \pm 0.003	0.989 \pm 0.002	0.930 \pm 0.003	0.947 \pm 0.013	0.969 \pm 0.002	0.974 \pm 0.000
credit	Shape	0.971 \pm 0.003	0.937 \pm 0.013	0.944 \pm 0.003	0.926 \pm 0.007	0.932 \pm 0.000	0.944 \pm 0.003	0.932 \pm 0.007	0.931 \pm 0.004	0.963 \pm 0.001	0.979 \pm 0.001	0.983 \pm 0.000
	Trend	0.925 \pm 0.004	0.862 \pm 0.030	0.894 \pm 0.005	0.864 \pm 0.007	0.861 \pm 0.000	0.896 \pm 0.006	0.862 \pm 0.008	0.848 \pm 0.004	0.903 \pm 0.002	0.933 \pm 0.003	0.946 \pm 0.000
diabetes	Shape	0.898 \pm 0.004	0.923 \pm 0.006	0.793 \pm 0.042	0.769 \pm 0.017	0.881 \pm 0.000	0.943 \pm 0.004	0.955 \pm 0.007	0.824 \pm 0.012	0.934 \pm 0.003	0.939 \pm 0.002	0.943 \pm 0.002
	Trend	0.949 \pm 0.007	0.898 \pm 0.004	0.913 \pm 0.001	0.875 \pm 0.003	0.921 \pm 0.000	0.952 \pm 0.005	0.964 \pm 0.002	0.858 \pm 0.008	0.965 \pm 0.004	0.967 \pm 0.001	0.970 \pm 0.004
iris	Shape	0.893 \pm 0.011	0.822 \pm 0.022	0.762 \pm 0.040	0.553 \pm 0.024	0.870 \pm 0.000	0.906 \pm 0.017	0.893 \pm 0.003	0.809 \pm 0.004	0.868 \pm 0.007	0.868 \pm 0.000	0.862 \pm 0.006
	Trend	0.897 \pm 0.007	0.590 \pm 0.019	0.793 \pm 0.047	0.506 \pm 0.036	0.899 \pm 0.000	0.896 \pm 0.016	0.917 \pm 0.007	0.783 \pm 0.017	0.931 \pm 0.004	0.942 \pm 0.005	0.934 \pm 0.002
qsar	Shape	0.931 \pm 0.004	0.917 \pm 0.003	0.891 \pm 0.001	0.602 \pm 0.005	0.887 \pm 0.000	0.959 \pm 0.003	0.930 \pm 0.005	0.873 \pm 0.007	0.940 \pm 0.001	0.947 \pm 0.000	0.948 \pm 0.000
	Trend	0.911 \pm 0.009	0.863 \pm 0.007	0.887 \pm 0.010	0.605 \pm 0.001	0.855 \pm 0.000	0.890 \pm 0.007	0.914 \pm 0.009	0.849 \pm 0.012	0.931 \pm 0.008	0.947 \pm 0.001	0.949 \pm 0.001
wdbc	Shape	0.923 \pm 0.003	0.861 \pm 0.005	0.824 \pm 0.031	0.395 \pm 0.017	0.873 \pm 0.000	0.945 \pm 0.006	0.946 \pm 0.004	0.749 \pm 0.026	0.951 \pm 0.001	0.975 \pm 0.001	0.972 \pm 0.003
	Trend	0.939 \pm 0.001	0.866 \pm 0.007	0.934 \pm 0.003	0.772 \pm 0.010	0.896 \pm 0.000	0.954 \pm 0.001	0.976 \pm 0.002	0.907 \pm 0.017	0.963 \pm 0.003	0.986 \pm 0.001	0.985 \pm 0.001
Avg.	Shape	0.925 \pm 0.038	0.898 \pm 0.067	0.852 \pm 0.059	0.751 \pm 0.224	0.881 \pm 0.059	0.929 \pm 0.065	0.931 \pm 0.054	0.860 \pm 0.062	0.913 \pm 0.050	0.927 \pm 0.051	0.929 \pm 0.052
	Trend	0.904 \pm 0.056	0.825 \pm 0.120	0.857 \pm 0.076	0.783 \pm 0.161	0.867 \pm 0.084	0.906 \pm 0.089	0.919 \pm 0.083	0.839 \pm 0.061	0.913 \pm 0.064	0.935 \pm 0.055	0.938 \pm 0.056

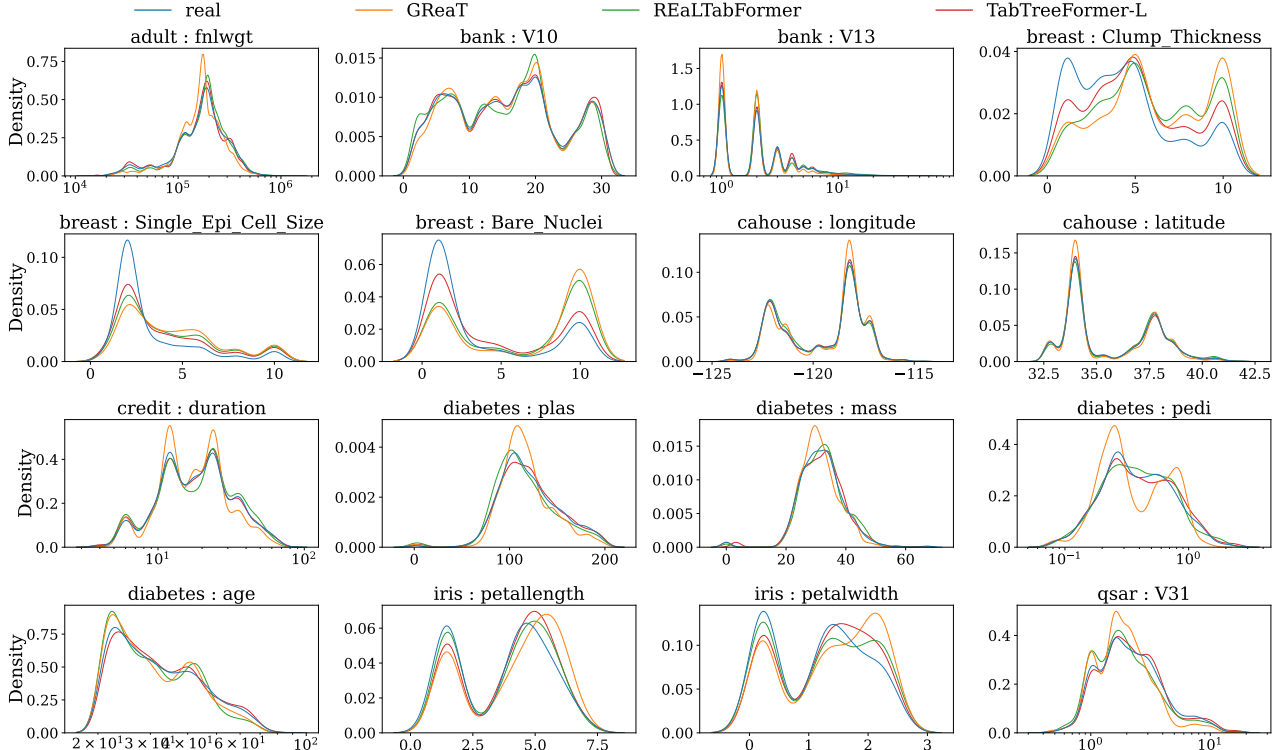


Figure 11. Visualization of the marginal densities of the generated data of baseline auto-regressive transformers and TabTreeFormer in comparison to the real data on some more representative multimodal-distributed continuous columns.

Table 10. Performance comparison between different models in terms of MLE. Classification tasks are evaluated by weighted AUC ROC scores, and regression tasks are evaluated by R^2 scores. The last row shows the average relative error versus real. The best scores and the second best scores are highlighted in bold with and without underscore, respectively. Equal values in the first 3 digits may be compared by the 4-th or 5-th digits.

Dataset	ML	real	ARF	CTAB+	CTGAN	TabDDPM	GReaT	RTF	TabSyn	TVAE	TTF-S	TTF-M	TTF-L
adult	LN	0.914	0.907 \pm 0.000	0.904 \pm 0.001	0.886 \pm 0.009	0.908 \pm 0.000	0.911 \pm 0.000	0.911 \pm 0.000	0.910 \pm 0.002	0.893 \pm 0.001	0.905 \pm 0.001	0.908 \pm 0.002	0.910 \pm 0.000
	RF	0.910	0.903 \pm 0.001	0.902 \pm 0.002	0.884 \pm 0.003	0.904 \pm 0.001	0.905 \pm 0.000	0.908 \pm 0.000	0.905 \pm 0.003	0.892 \pm 0.001	0.900 \pm 0.000	0.905 \pm 0.000	0.906 \pm 0.001
	XGB	0.914	0.907 \pm 0.001	0.905 \pm 0.001	0.886 \pm 0.002	0.908 \pm 0.000	0.911 \pm 0.000	0.912 \pm 0.001	0.910 \pm 0.003	0.895 \pm 0.001	0.904 \pm 0.000	0.909 \pm 0.001	0.911 \pm 0.001
bank	LN	0.907	0.895 \pm 0.002	0.901 \pm 0.003	0.887 \pm 0.003	0.900 \pm 0.002	0.907 \pm 0.000	0.904 \pm 0.000	0.900 \pm 0.005	0.890 \pm 0.005	0.894 \pm 0.005	0.905 \pm 0.001	0.902 \pm 0.001
	RF	0.930	0.900 \pm 0.001	0.902 \pm 0.002	0.882 \pm 0.002	0.908 \pm 0.001	0.907 \pm 0.001	0.913 \pm 0.001	0.907 \pm 0.006	0.884 \pm 0.002	0.893 \pm 0.011	0.916 \pm 0.002	0.921 \pm 0.001
	XGB	0.936	0.903 \pm 0.005	0.906 \pm 0.000	0.884 \pm 0.002	0.912 \pm 0.001	0.910 \pm 0.001	0.918 \pm 0.002	0.913 \pm 0.007	0.885 \pm 0.001	0.890 \pm 0.012	0.919 \pm 0.000	0.927 \pm 0.003
boston	LN	0.590	0.451 \pm 0.021	0.264 \pm 0.034	0.374 \pm 0.075	0.000 \pm 1.391	0.397 \pm 0.000	0.529 \pm 0.028	0.533 \pm 0.036	0.480 \pm 0.030	0.541 \pm 0.024	0.573 \pm 0.001	0.577 \pm 0.002
	RF	0.662	0.484 \pm 0.057	0.129 \pm 0.015	0.336 \pm 0.089	0.000 \pm 1.288	0.281 \pm 0.001	0.584 \pm 0.006	0.658 \pm 0.025	0.287 \pm 0.032	0.634 \pm 0.028	0.727 \pm 0.009	0.738 \pm 0.004
	XGB	0.701	0.509 \pm 0.067	0.097 \pm 0.073	0.364 \pm 0.103	0.000 \pm 1.128	0.277 \pm 0.014	0.578 \pm 0.056	0.647 \pm 0.017	0.284 \pm 0.082	0.653 \pm 0.022	0.677 \pm 0.023	0.680 \pm 0.003
breast	LN	0.985	0.984 \pm 0.005	0.913 \pm 0.091	0.978 \pm 0.001	0.985 \pm 0.002	0.985 \pm 0.000	0.987 \pm 0.002	0.987 \pm 0.001	0.930 \pm 0.009	0.985 \pm 0.003	0.985 \pm 0.001	0.984 \pm 0.001
	RF	0.985	0.982 \pm 0.003	0.968 \pm 0.012	0.985 \pm 0.003	0.981 \pm 0.002	0.979 \pm 0.004	0.980 \pm 0.000	0.981 \pm 0.002	0.976 \pm 0.007	0.985 \pm 0.002	0.986 \pm 0.001	0.985 \pm 0.001
	XGB	0.984	0.979 \pm 0.001	0.958 \pm 0.025	0.984 \pm 0.002	0.981 \pm 0.001	0.982 \pm 0.002	0.982 \pm 0.002	0.987 \pm 0.001	0.981 \pm 0.005	0.984 \pm 0.002	0.981 \pm 0.000	0.985 \pm 0.001
cahouse	LN	0.653	0.620 \pm 0.003	0.604 \pm 0.015	0.561 \pm 0.019	0.577 \pm 0.013	0.646 \pm 0.000	0.649 \pm 0.001	0.640 \pm 0.002	0.605 \pm 0.002	0.625 \pm 0.004	0.645 \pm 0.005	0.648 \pm 0.003
	RF	0.822	0.712 \pm 0.010	0.641 \pm 0.015	0.594 \pm 0.016	0.743 \pm 0.002	0.776 \pm 0.003	0.799 \pm 0.002	0.771 \pm 0.003	0.679 \pm 0.004	0.700 \pm 0.009	0.774 \pm 0.012	0.801 \pm 0.002
	XGB	0.836	0.737 \pm 0.015	0.664 \pm 0.008	0.605 \pm 0.015	0.769 \pm 0.003	0.792 \pm 0.003	0.819 \pm 0.001	0.792 \pm 0.003	0.700 \pm 0.003	0.708 \pm 0.009	0.792 \pm 0.015	0.814 \pm 0.003
credit	LN	0.836	0.773 \pm 0.064	0.538 \pm 0.093	0.814 \pm 0.012	0.781 \pm 0.018	0.665 \pm 0.000	0.801 \pm 0.006	0.780 \pm 0.017	0.702 \pm 0.042	0.823 \pm 0.022	0.823 \pm 0.010	0.822 \pm 0.006
	RF	0.837	0.769 \pm 0.030	0.505 \pm 0.097	0.782 \pm 0.033	0.755 \pm 0.013	0.722 \pm 0.014	0.820 \pm 0.010	0.791 \pm 0.007	0.746 \pm 0.057	0.811 \pm 0.015	0.796 \pm 0.008	0.795 \pm 0.004
	XGB	0.844	0.788 \pm 0.019	0.509 \pm 0.088	0.788 \pm 0.023	0.748 \pm 0.026	0.739 \pm 0.006	0.797 \pm 0.039	0.795 \pm 0.014	0.759 \pm 0.048	0.816 \pm 0.015	0.811 \pm 0.016	0.801 \pm 0.020
diabetes	LN	0.884	0.854 \pm 0.014	0.817 \pm 0.028	0.864 \pm 0.017	0.753 \pm 0.032	0.858 \pm 0.000	0.878 \pm 0.005	0.883 \pm 0.006	0.863 \pm 0.008	0.889 \pm 0.002	0.884 \pm 0.001	0.885 \pm 0.003
	RF	0.869	0.818 \pm 0.023	0.802 \pm 0.014	0.818 \pm 0.008	0.838 \pm 0.024	0.824 \pm 0.012	0.841 \pm 0.010	0.844 \pm 0.012	0.817 \pm 0.020	0.865 \pm 0.009	0.864 \pm 0.006	0.854 \pm 0.009
	XGB	0.867	0.838 \pm 0.012	0.811 \pm 0.005	0.807 \pm 0.005	0.832 \pm 0.017	0.831 \pm 0.003	0.849 \pm 0.010	0.847 \pm 0.009	0.820 \pm 0.020	0.863 \pm 0.006	0.849 \pm 0.008	0.850 \pm 0.012
Avg.	RE	-	0.057 \pm 0.077	0.244 \pm 0.274	0.099 \pm 0.137	0.483 \pm 1.214	0.110 \pm 0.170	0.027 \pm 0.040	0.027 \pm 0.029	0.095 \pm 0.142	0.029 \pm 0.040	0.017 \pm 0.023	0.016 \pm 0.023

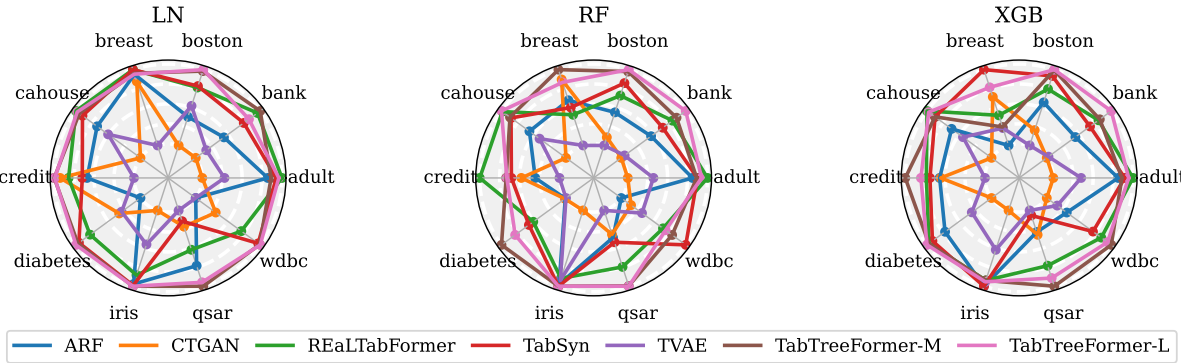


Figure 12. Performance comparison between different models in terms of MLE. Top-5 performing baselines by average MLE relative errors are visualized. LN, RF, and XGB are the ML model names.

D.6. Raw Results for Ablation Study

Table 14 shows the raw results for ablation study.

E. Comparison to Baselines without Public Code

There are two recent tabular data generation works, TabMT (Gulati & Roysdon, 2023) and TabDiff (Shi et al., 2024), that have not published their code by the time of the composition of this paper. Unfortunately, although all pa-

Table 11. Performance comparison between different models in terms of DCR. p -values less than 0.05 is highlighted in red, indicating a high risk of privacy leakage.

Dataset	ARF	CTAB+	CTGAN	TabDDPM	GReAT	RTF	TabSyn	TVAE	TTF-S	TTF-M	TTF-L
adult	0.486 \pm 0.077	0.691 \pm 0.424	0.687 \pm 0.272	0.440 \pm 0.125	0.000\pm0.000	0.139 \pm 0.131	0.654 \pm 0.149	0.003\pm0.004	0.999 \pm 0.001	0.992 \pm 0.011	0.993 \pm 0.006
bank	0.999 \pm 0.000	0.849 \pm 0.093	0.996 \pm 0.003	0.873 \pm 0.077	0.040\pm0.000	0.812 \pm 0.073	0.938 \pm 0.027	0.709 \pm 0.377	0.973 \pm 0.006	0.811 \pm 0.031	0.836 \pm 0.108
boston	0.179 \pm 0.084	0.099 \pm 0.071	0.272 \pm 0.192	0.539 \pm 0.242	0.035\pm0.000	0.261 \pm 0.075	0.333 \pm 0.377	0.060 \pm 0.031	0.240 \pm 0.251	0.440 \pm 0.019	0.421 \pm 0.039
breast	0.071 \pm 0.060	0.333 \pm 0.468	0.595 \pm 0.415	0.039\pm0.026	0.005\pm0.000	0.165 \pm 0.193	0.357 \pm 0.256	1.000 \pm 0.000	0.045\pm0.002	0.061 \pm 0.019	0.111 \pm 0.071
cahouse	0.147 \pm 0.038	0.349 \pm 0.246	0.131 \pm 0.185	0.036\pm0.005	0.001\pm0.000	0.097 \pm 0.073	0.151 \pm 0.120	0.062 \pm 0.035	0.087 \pm 0.058	0.673 \pm 0.209	0.340 \pm 0.157
credit	0.197 \pm 0.068	0.161 \pm 0.124	0.462 \pm 0.131	0.725 \pm 0.261	0.990 \pm 0.000	0.300 \pm 0.120	0.689 \pm 0.246	0.581 \pm 0.194	0.270 \pm 0.077	0.289 \pm 0.121	0.381 \pm 0.043
diabetes	0.698 \pm 0.230	0.890 \pm 0.036	0.835 \pm 0.187	0.990 \pm 0.005	0.971 \pm 0.000	0.870 \pm 0.147	0.825 \pm 0.093	0.909 \pm 0.049	0.887 \pm 0.078	0.762 \pm 0.044	0.727 \pm 0.036
iris	0.796 \pm 0.127	0.970 \pm 0.039	0.932 \pm 0.032	0.972 \pm 0.038	0.187 \pm 0.000	0.654 \pm 0.353	0.765 \pm 0.149	0.770 \pm 0.118	0.363 \pm 0.176	0.343 \pm 0.124	0.570 \pm 0.118
qsar	0.668 \pm 0.231	0.546 \pm 0.193	0.669 \pm 0.186	0.485 \pm 0.306	0.063 \pm 0.000	0.750 \pm 0.072	0.664 \pm 0.238	0.351 \pm 0.160	0.794 \pm 0.120	0.951 \pm 0.026	0.952 \pm 0.006
wdbc	0.821 \pm 0.029	0.647 \pm 0.283	0.909 \pm 0.068	1.000 \pm 0.000	0.591 \pm 0.000	0.784 \pm 0.111	0.853 \pm 0.096	0.307 \pm 0.170	0.911 \pm 0.051	0.977 \pm 0.008	0.956 \pm 0.012

Table 12. Performance comparison between different models in terms of RDD. AUC-ROC scores are reported, the smaller values mean that the synthetic records are harder to be detected. The best scores and the second best scores are highlighted in bold with and without underscore, respectively. Equal values in the first 3 digits may be compared by the 4-th or 5-th digits.

Dataset	ML	ARF	CTAB+	CTGAN	TabDDPM	GReAT	RTF	TabSyn	TVAE	TTF-S	TTF-M	TTF-L
adult	LN	0.794 \pm 0.006	0.632 \pm 0.016	0.946 \pm 0.005	0.585\pm0.005	0.714 \pm 0.000	0.602\pm0.000	0.614 \pm 0.031	0.945 \pm 0.003	0.852 \pm 0.001	0.836 \pm 0.001	0.830 \pm 0.001
	RF	0.877 \pm 0.003	0.711 \pm 0.010	0.983 \pm 0.007	0.739 \pm 0.002	0.741 \pm 0.001	0.605\pm0.002	0.691\pm0.067	0.978 \pm 0.005	0.871 \pm 0.002	0.868 \pm 0.007	0.858 \pm 0.002
	XGB	0.902 \pm 0.003	0.734 \pm 0.011	0.989 \pm 0.004	0.762 \pm 0.002	0.758 \pm 0.001	0.617\pm0.002	0.714\pm0.068	0.985 \pm 0.003	0.894 \pm 0.002	0.874 \pm 0.004	0.859 \pm 0.001
bank	LN	0.736 \pm 0.004	0.607 \pm 0.013	0.818 \pm 0.013	0.581\pm0.004	0.700 \pm 0.000	0.613 \pm 0.001	0.588 \pm 0.025	0.826 \pm 0.021	0.664 \pm 0.017	0.608 \pm 0.010	0.578\pm0.006
	RF	0.869 \pm 0.014	0.745 \pm 0.007	0.961 \pm 0.006	0.783 \pm 0.003	0.824 \pm 0.000	0.668\pm0.002	0.742\pm0.060	0.968 \pm 0.006	0.995 \pm 0.001	0.991 \pm 0.001	0.990 \pm 0.000
	XGB	0.901 \pm 0.008	0.795 \pm 0.008	0.980 \pm 0.002	0.821 \pm 0.007	0.842 \pm 0.001	0.704\pm0.002	0.784\pm0.038	0.983 \pm 0.002	0.997 \pm 0.001	0.992 \pm 0.001	0.990 \pm 0.000
boston	LN	0.579 \pm 0.019	0.741 \pm 0.041	0.830 \pm 0.075	0.994 \pm 0.004	0.674 \pm 0.000	0.583 \pm 0.025	0.625 \pm 0.026	0.614 \pm 0.014	0.547 \pm 0.040	0.578\pm0.006	0.568\pm0.007
	RF	0.938 \pm 0.014	0.994 \pm 0.002	0.993 \pm 0.003	1.000 \pm 0.000	0.884\pm0.002	0.651\pm0.011	0.963 \pm 0.026	0.993 \pm 0.002	0.995 \pm 0.003	0.986 \pm 0.004	0.987 \pm 0.005
	XGB	0.922 \pm 0.017	0.995 \pm 0.001	0.993 \pm 0.005	1.000 \pm 0.000	0.862\pm0.016	0.642\pm0.005	0.978 \pm 0.010	0.996 \pm 0.001	0.996 \pm 0.002	0.993 \pm 0.007	0.995 \pm 0.003
breast	LN	0.605 \pm 0.006	0.723 \pm 0.014	0.690 \pm 0.040	0.619 \pm 0.013	0.685 \pm 0.000	0.658 \pm 0.020	0.695 \pm 0.032	0.702 \pm 0.046	0.615 \pm 0.005	0.573\pm0.012	0.582\pm0.020
	RF	0.615 \pm 0.014	0.921 \pm 0.041	0.743 \pm 0.021	0.623 \pm 0.006	0.668 \pm 0.001	0.659 \pm 0.013	0.670 \pm 0.019	0.823 \pm 0.012	0.598 \pm 0.006	0.586\pm0.011	0.586\pm0.016
	XGB	0.604 \pm 0.011	0.922 \pm 0.041	0.751 \pm 0.026	0.611 \pm 0.005	0.652 \pm 0.017	0.650 \pm 0.024	0.700 \pm 0.018	0.850 \pm 0.017	0.577 \pm 0.005	0.556\pm0.009	0.568\pm0.016
cahouse	LN	0.517\pm0.003	0.636 \pm 0.063	0.697 \pm 0.017	0.523 \pm 0.005	0.605 \pm 0.000	0.538 \pm 0.002	0.515\pm0.004	0.584 \pm 0.017	0.576 \pm 0.010	0.538 \pm 0.002	0.520 \pm 0.005
	RF	0.926 \pm 0.003	0.934 \pm 0.007	0.968 \pm 0.011	0.896 \pm 0.003	0.771\pm0.001	0.658\pm0.019	0.949 \pm 0.002	0.940 \pm 0.002	0.936 \pm 0.006	0.875 \pm 0.013	0.816 \pm 0.038
	XGB	0.923 \pm 0.004	0.967 \pm 0.007	0.987 \pm 0.003	0.864 \pm 0.001	0.778\pm0.001	0.672\pm0.015	0.891 \pm 0.010	0.969 \pm 0.003	0.985 \pm 0.001	0.934 \pm 0.006	0.903 \pm 0.001
credit	LN	0.505 \pm 0.007	0.634 \pm 0.066	0.654 \pm 0.035	0.663 \pm 0.013	0.708 \pm 0.000	0.639 \pm 0.016	0.812 \pm 0.034	0.688 \pm 0.027	0.658 \pm 0.028	0.485\pm0.018	0.491\pm0.002
	RF	0.858 \pm 0.003	0.910 \pm 0.074	0.917 \pm 0.017	0.794 \pm 0.026	0.816 \pm 0.001	0.655 \pm 0.016	0.785 \pm 0.038	0.921 \pm 0.011	0.669 \pm 0.023	0.522\pm0.015	0.564\pm0.010
	XGB	0.866 \pm 0.004	0.920 \pm 0.083	0.927 \pm 0.013	0.799 \pm 0.021	0.835 \pm 0.005	0.678 \pm 0.010	0.856 \pm 0.017	0.942 \pm 0.008	0.707 \pm 0.036	0.540\pm0.005	0.526\pm0.010
diabetes	LN	0.547\pm0.009	0.629 \pm 0.045	0.767 \pm 0.026	0.714 \pm 0.012	0.727 \pm 0.000	0.605 \pm 0.009	0.469\pm0.021	0.573 \pm 0.018	0.502 \pm 0.036	0.550 \pm 0.012	0.570 \pm 0.014
	RF	0.725 \pm 0.021	0.845 \pm 0.016	0.924 \pm 0.038	0.865 \pm 0.017	0.811 \pm 0.001	0.610\pm0.022	0.603\pm0.022	0.953 \pm 0.009	0.743 \pm 0.015	0.713 \pm 0.004	0.753 \pm 0.005
	XGB	0.754 \pm 0.018	0.844 \pm 0.014	0.948 \pm 0.019	0.868 \pm 0.011	0.814 \pm 0.003	0.659\pm0.027	0.706\pm0.012	0.977 \pm 0.009	0.722 \pm 0.012	0.722 \pm 0.022	0.738 \pm 0.007
iris	LN	0.518 \pm 0.077	0.796 \pm 0.040	0.867 \pm 0.002	0.806 \pm 0.111	0.534 \pm 0.000	0.619 \pm 0.049	0.485 \pm 0.081	0.510 \pm 0.055	0.494 \pm 0.048	0.433\pm0.037	0.473\pm0.050
	RF	0.877 \pm 0.023	0.989 \pm 0.008	0.969 \pm 0.007	0.999 \pm 0.002	0.628\pm0.029	0.549\pm0.084	0.896 \pm 0.067	0.954 \pm 0.014	0.988 \pm 0.012	0.996 \pm 0.003	0.969 \pm 0.005
	XGB	0.931 \pm 0.037	0.984 \pm 0.010	0.944 \pm 0.003	0.998 \pm 0.003	0.570\pm0.009	0.613\pm0.037	0.896 \pm 0.052	0.975 \pm 0.006	0.992 \pm 0.005	0.997 \pm 0.002	0.981 \pm 0.022
qsar	LN	0.659 \pm 0.025	0.838 \pm 0.031	0.930 \pm 0.013	1.000 \pm 0.000	0.821 \pm 0.000	0.582 \pm 0.022	0.770 \pm 0.016	0.801 \pm 0.034	0.542 \pm 0.013	0.522\pm0.004	0.531\pm0.005
	RF	0.972 \pm 0.006	1.000 \pm 0.000	0.999 \pm 0.001	1.000 \pm 0.000	0.979 \pm 0.001	0.677\pm0.053	0.946\pm0.018	0.998 \pm 0.001	0.995 \pm 0.001	0.968 \pm 0.011	0.976 \pm 0.007
	XGB	0.984 \pm 0.007	1.000 \pm 0.000	0.999 \pm 0.000	1.000 \pm 0.000	0.989 \pm 0.002	0.761\pm0.014	0.975\pm0.003	0.998 \pm 0.001	0.997 \pm 0.001	0.999 \pm 0.002	0.998 \pm 0.000
wdbc	LN	0.517\pm0.008	0.832 \pm 0.049	0.961 \pm 0.020	0.994 \pm 0.004	0.675 \pm 0.000	0.564 \pm 0.060	0.658 \pm 0.018	0.743 \pm 0.024	0.550 \pm 0.033	0.511\pm0.005	0.521 \pm 0.016
	RF	0.948 \pm 0.007	1.000 \pm 0.000	0.993 \pm 0.006	1.000 \pm 0.000	0.965 \pm 0.003	0.695 \pm 0.046	0.616 \pm 0.057	0.989 \pm 0.001			

Table 13. Comparison between different models in terms of time taken for training and generation. The values are in unit of seconds.

Dataset	Action	ARF	CTAB+	CTGAN	TabDDPM	GReaT	RTF	TabSyn	TVAE	TTF-S	TTF-M	TTF-L
adult	Train	258.758 \pm 0.030	787.379 \pm 3.334	753.259 \pm 104.080	285.153 \pm 0.410	10397.040 \pm 9.203	1875.904 \pm 34.663	1199.823 \pm 146.744	1111.927 \pm 2.790	166.807 \pm 31.955	235.554 \pm 71.542	606.790 \pm 277.828
	Generate	41.029 \pm 0.363	0.429 \pm 0.001	0.112 \pm 0.001	63.388 \pm 0.083	138.023 \pm 0.205	89.460 \pm 4.301	2.409 \pm 0.010	0.357 \pm 0.005	30.822 \pm 3.553	35.275 \pm 6.059	96.027 \pm 37.920
bank	Train	121.480 \pm 39.164	737.314 \pm 0.138	544.578 \pm 62.697	252.016 \pm 0.266	10295.769 \pm 21.720	835.167 \pm 1.619	1865.473 \pm 418.665	878.170 \pm 122.998	228.772 \pm 62.554	225.707 \pm 39.181	744.726 \pm 221.487
	Generate	42.208 \pm 5.408	1.126 \pm 0.006	0.733 \pm 0.001	55.038 \pm 0.077	149.872 \pm 0.104	106.036 \pm 0.080	3.009 \pm 0.006	0.975 \pm 0.003	36.731 \pm 3.457	37.163 \pm 3.021	117.167 \pm 30.088
boston	Train	1.184 \pm 0.368	8.396 \pm 0.048	14.945 \pm 5.245	4.499 \pm 0.047	121.619 \pm 0.090	49.693 \pm 3.175	862.625 \pm 48.241	7.158 \pm 0.387	94.498 \pm 42.830	224.217 \pm 30.311	432.354 \pm 180.912
	Generate	1.184 \pm 0.269	0.083 \pm 0.001	0.062 \pm 0.000	2.332 \pm 0.459	2.422 \pm 0.003	3.059 \pm 0.003	0.156 \pm 0.003	0.066 \pm 0.000	0.372 \pm 0.094	0.694 \pm 0.055	1.275 \pm 0.379
breast	Train	0.585 \pm 0.015	8.479 \pm 0.026	13.571 \pm 2.035	6.136 \pm 0.099	153.352 \pm 0.134	25.537 \pm 1.419	1037.126 \pm 281.166	6.340 \pm 0.925	64.589 \pm 26.284	207.280 \pm 0.096	537.723 \pm 206.786
	Generate	0.876 \pm 0.013	0.056 \pm 0.008	0.051 \pm 0.000	3.123 \pm 0.007	3.434 \pm 0.016	0.759 \pm 0.003	0.249 \pm 0.003	0.055 \pm 0.000	0.315 \pm 0.050	0.527 \pm 0.002	1.315 \pm 0.403
cahouse	Train	109.471 \pm 13.706	280.228 \pm 0.142	311.628 \pm 21.038	96.491 \pm 0.350	4373.950 \pm 56.089	596.523 \pm 51.206	1838.247 \pm 200.652	208.611 \pm 25.684	267.307 \pm 29.842	340.992 \pm 76.571	946.903 \pm 102.584
	Generate	8.087 \pm 0.220	0.839 \pm 0.016	0.690 \pm 0.011	16.056 \pm 0.012	57.584 \pm 0.061	69.522 \pm 0.044	2.676 \pm 0.000	0.787 \pm 0.000	7.774 \pm 0.457	9.725 \pm 1.549	29.610 \pm 2.509
credit	Train	2.262 \pm 0.089	8.400 \pm 0.035	32.463 \pm 8.548	8.102 \pm 0.215	277.555 \pm 0.388	63.648 \pm 0.758	726.006 \pm 67.662	13.246 \pm 1.809	152.310 \pm 23.655	250.729 \pm 75.271	446.486 \pm 161.523
	Generate	2.198 \pm 0.088	0.043 \pm 0.000	0.035 \pm 0.000	4.526 \pm 0.007	5.845 \pm 0.008	2.407 \pm 0.171	0.167 \pm 0.003	0.041 \pm 0.000	0.541 \pm 0.153	1.062 \pm 0.179	2.018 \pm 0.586
diabetes	Train	1.100 \pm 0.094	8.524 \pm 0.407	20.414 \pm 2.831	5.799 \pm 1.191	130.793 \pm 0.077	37.372 \pm 3.118	758.140 \pm 41.333	7.944 \pm 1.272	69.127 \pm 35.429	74.799 \pm 18.217	560.410 \pm 149.115
	Generate	0.943 \pm 0.047	0.047 \pm 0.001	0.036 \pm 0.000	2.329 \pm 0.822	1.496 \pm 0.008	1.504 \pm 0.007	0.139 \pm 0.000	0.039 \pm 0.000	0.412 \pm 0.044	0.427 \pm 0.023	1.580 \pm 0.318
iris	Train	0.153 \pm 0.002	7.267 \pm 0.021	6.538 \pm 0.504	3.485 \pm 0.210	24.975 \pm 0.018	15.369 \pm 1.242	620.864 \pm 35.603	2.811 \pm 0.518	225.728 \pm 194.228	406.082 \pm 0.376	482.266 \pm 0.176
	Generate	0.690 \pm 0.010	0.033 \pm 0.006	0.016 \pm 0.000	6.208 \pm 2.124	0.360 \pm 0.015	0.225 \pm 0.001	0.098 \pm 0.002	0.016 \pm 0.001	0.124 \pm 0.054	0.198 \pm 0.000	0.331 \pm 0.010
qsar	Train	18.992 \pm 1.983	18.389 \pm 0.217	64.331 \pm 11.582	7.369 \pm 0.156	566.658 \pm 23.451	152.950 \pm 0.819	694.890 \pm 76.489	23.013 \pm 2.183	132.603 \pm 45.722	297.779 \pm 59.962	739.373 \pm 278.301
	Generate	2.842 \pm 0.012	0.206 \pm 0.006	0.192 \pm 0.000	2.825 \pm 0.826	46.712 \pm 3.062	10.997 \pm 0.072	0.336 \pm 0.005	0.203 \pm 0.001	1.059 \pm 0.032	2.375 \pm 0.210	5.404 \pm 1.685
wdbc	Train	5.344 \pm 0.860	10.795 \pm 0.089	24.175 \pm 7.507	4.249 \pm 0.056	265.340 \pm 2.411	183.908 \pm 1.047	631.546 \pm 68.079	9.356 \pm 1.238	132.480 \pm 48.560	235.600 \pm 110.069	504.627 \pm 29.714
	Generate	1.410 \pm 0.007	0.159 \pm 0.001	0.154 \pm 0.002	1.934 \pm 0.010	65.821 \pm 1.106	9.936 \pm 0.017	0.276 \pm 0.000	0.159 \pm 0.000	0.606 \pm 0.019	1.252 \pm 0.180	2.231 \pm 0.084
Avg.	Train	51.933 \pm 86.361	187.517 \pm 314.694	178.590 \pm 268.489	67.330 \pm 110.073	2660.705 \pm 4255.243	383.607 \pm 593.187	1023.474 \pm 472.880	226.858 \pm 413.306	153.422 \pm 69.440	249.874 \pm 87.633	600.166 \pm 163.582
	Generate	10.147 \pm 16.730	0.302 \pm 0.384	0.208 \pm 0.271	15.776 \pm 23.351	47.157 \pm 66.920	29.391 \pm 41.741	0.952 \pm 0.216	0.270 \pm 0.341	7.876 \pm 13.911	8.870 \pm 14.692	25.696 \pm 43.802

Table 14. Ablation studies.

Dataset	ML	credit			diabetes		
		LN	RF	XGB	LN	RF	XGB
TTF		0.823 \pm 0.022	0.811 \pm 0.014	0.816 \pm 0.015	0.889 \pm 0.002	0.865 \pm 0.009	0.863 \pm 0.006
w/o TBM		0.761 \pm 0.030	0.747 \pm 0.023	0.726 \pm 0.047	0.880 \pm 0.002	0.848 \pm 0.004	0.824 \pm 0.010
w/o DQT		0.725 \pm 0.013	0.807 \pm 0.002	0.813 \pm 0.010	0.881 \pm 0.002	0.863 \pm 0.007	0.861 \pm 0.002
w/o OCEL		0.839 \pm 0.009	0.813 \pm 0.024	0.815 \pm 0.017	0.881 \pm 0.002	0.847 \pm 0.006	0.839 \pm 0.007

similar margin, and wins over REaLTabFormer by a lower margin. Moreover, the results for REaLTabFormer reported by TabMT are not done by reproduced experiments, but directly taken from REaLTabFormer paper. Experiments done separately, possibly on different splits, may result in a non-negligible change in the MLE scores, which is also acknowledged by TabMT authors. In addition, TabMT’s result is reported on 15 datasets while REaLTabFormer’s result is reported on 6 datasets only, and the 6 datasets reported for REaLTabFormer are harder than the rest 9 datasets by a higher MLE relative error over all the other reported baselines in that paper. Therefore, TabTreeFormer is likely to outperform TabMT.

TabDiff. TabTreeFormer wins over *all* the reported baselines with a greater margin. Thus, it is also very likely that TabTreeFormer outperforms TabDiff.

F. Limitations and Future Work

Optimizing tree-based model. TabTreeFormer uses LightGBM fitted on the target column to introduce tabular inductive biases from tree-based models. While this is effective and easy to implement, modified tree-based models catered for guiding the generation may further improve the performance, such as using trees from a generative tree-based model (e.g. ARF), and selecting a better target column using some heuristics.

Optimizing de-quantization of tokenization. The dual-quantization tokenization may be further optimized with some sampling around the quantile values if use case requires smoother values in continuous values (e.g. for RDD evaluation, recall Appendix D.4).

Masked vs. Auto-regressive transformers. TabMT has demonstrated the effectiveness of a masked transformer with iterative decoding for tabular data generation, but TabMT does not provide ablation study result on masked vs. auto-

regressive transformers. Thus, this approach may be used in place of a causal language model to further improve synthetic data quality. Further exploration could be useful.

Extension to general tabular models. The idea of introducing tree-based models to transformers on tabular data may not be limited to generation task, but also applies to tasks like classification and regression. Future works may explore the extendiblity of this idea to other tasks.